Journal of the Geological Survey of Brazil

Geochemistry of the upper estuarine sediments of the Santos estuary, São Paulo Brazil: provenance and anthropogenic pollution

Bruno de Oliveira Calado[1], Colombo Celso Gaeta Tassinari[2]

[1]Serviço Geológico do Brasil – CPRM, Av. Antônio Sales, 1418, Joaquim Távora, Fortaleza – CE, CEP:60135-101
[2]Instituto de Geociências – USP, Rua do Lago, 562, Butantã, São Paulo – SP, CEP:05508-080

Abstract

Major and trace element geochemistry of the upper estuarine sediments of the Santos estuary has been used to characterize sediment geochemistry, classification, distribution, and possible sources of industrial pollution. The vertical sediment cores were collected on the margin of the Cubatão, Perequê, Mogi, Piaçaguera and Jurubatuba rivers, the main effluents of the Santos estuarine system. Samples of selected basement rocks (n=12), industrial waste (n=2) and one weathering profile (organic soil, residual soil and saprolite rock) were also analyzed. The sedimentary deposits showed interbedding of medium, fine, and very fine sands in the upper portion of the estuary and subordinate silt-clay units derived from lower energy in swamp/mangroves deposits in the lower estuary. Marked geochemical differences occurred among these fluvial sediments. The calculated indices of chemical weathering, such as Chemical Index of Alteration (CIA) and A-CN-K ternary diagram indicate that the estuarine sediments display a wide range of weathering effects, from unweathered derived of Proterozoic gneiss and granitic rocks to intensely weathered site in the swamp deposits of the Piaçaguera River.

Phosphogypsum waste stored in the catchment area of the Mogi River showed high concentrations of S, La, Ce, Ca, Sr, Nd, Nb, U, Ba, P, Y and F when compared with the regional rocks, soils and fluvial sediments samples analyzed in the study area, which make it a potential source of environmental contamination. The UCC-normalized patterns, geoaccumulation indexes (Igeo), robust linear regression (RA) and principal component analysis (PCA) were used to identify geochemical anomalies and discuss their probable sources. The principal component scores exhibited strong spatial association with anthropogenic sources. The principal component loading allowed to separate heavy metal elements (Cr, Cu, Ni, Pb and Zn) from the elements related to phosphogypsum waste (e.g., Ce, La, Nd and F). The geochemical anomalies of Ce, La, Nd and F in the fluvial sediments of the Mogi downstream River may be related to phosphogypsum waste in the catchment area, whereas the Cr, Cu and Ni anomalies may be related to fossil fuel, chemical industries and industrial waste deposits which occur near the Pereque and Cubatão rivers.

Article Information

Publication type: Research papers
Received 1 June 2020
Accepted 29 October 2020
Online pub.18 December 2020
Editor: Luciano Cunha

Keywords:
Sediment geochemistry;
Phosphogypsum waste;
Santos-São Vicente estuary;
anthropogenic pollution.

*Corresponding author
Bruno de Oliveira Calado
E-mail address: bruno.calado@cprm.gov.br

1. Introduction

Studies on chemical and particulate matter pollution are of great importance to quantify probable risks to human health and ecosystem (CETESB 1985; Spektor et al. 1991; Furlan 1998; Klumpp et al. 1996; Gutberlet 1997; Rizzio et al. 2001; Borrego et al. 2007; Tagawa et al. 2009; Ogundele et al. 2017; Zhang and Zhou 2020; Bontempi 2020), especially in industrialized and urban areas (Lü et al. 2019). Fertilizer and refinery industries located in Cubatão – Vila Parisi have been responsible, in the past, for the emission of a significant amount of suspended particulate matter with high levels of Si and F (CETESB 1985). Atmospheric fluoride is a highly phytotoxic atmospheric pollutant, and it was responsible for the degradation of the Serra do Mar vegetation in Cubatão, which favored the occurrence of landslides (CETESB 2018). Historical atmospheric fluoride rates showed decreased concentrations, especially in the Mogi Valley. However, the highest rate of fluoride in 2016 occurred in the northwestern portion of Mogi Valley, where the largest leaf accumulation of this pollutant was found using active biomonitoring. Although the condition has improved, there is still high potential for phytotoxicity (CETESB 2018). Some gaseous and particulate fluorides are assumed to play an important role in forest decline (Gutberlet 1997; Klumpp et al. 1996; Tagawa et al. 2009).

The Santos estuarine system is the main Brazilian example of environmental degradation owing to the activity of its harbours, steel industry, oil refineries and chemical

ISSN: 2595-1939
https://doi.org/10.29396/jgsb.2020.v3.n3.4
Open access at jgsb.cprm.gov.br

industries (CETESB 2001; Pires 2012), which are located in close proximity to mangroves and other protected areas. The Mogi Valley, located in the upper portion of the Santos estuary (Vila Parisi - Cubatão) (Fig. 1), is contaminated by open pit phosphogypsum waste stored in the watershed area (CETESB 2001; Borges 2003; Silva 2004; Fávaro 2005; Oliveira et al. 2007; Calado 2008). Phosphogypsum waste is enriched in rare-earth elements, particularly Ce, Eu, La, Nd, Sm, and Tb, and the elements Ba and Ta (Santos et al. 2002; Oliveira et al. 2007). This waste is classified as non-hazardous, non-inert waste (Class IIA), with As, F, Al, Fe, Mn and sulfate concentrations above the maximum limit established by the ABNT Standard 10004/2004 in the solubilization test (Jacomino et al. 2009). Industrial waste disposal can pollute and contaminate waters (Means et al. 1978; Bourg 1988; Santos et al. 2002; Papaslioti et al. 2020) and also adsorbed by aerosol particles and transported to surrounding areas (Borrego et al. 2007; Torres-Sánchez et al. 2020). A detailed evaluation of the chemical composition of industrial waste is necessary to determine effective waste management strategies (Vásconez-Maza et al. 2019).

In this study, the geochemistry of sediment cores in the upper portion of the Santos-São Vicente estuarine system was investigated in order to discriminate natural and/or anthropogenic sources of trace elements. To this end, we applied techniques such as geoaccumulation indexes (Igeo), UCC-normalized data, robust linear regression (RA) and principal component analysis (PCA) to better understand geochemical data. In addition, we applied the Chemical Index of Alteration (CIA), the A-CN-K ternary diagram and the terrigenous sediment classification (SandClass of Herron) to discuss sediment sources and fractionation processes in surface dynamics.

2. Study area

The Santos estuarine system is located on the coast of São Paulo state; it is bordered on the north by mountains of Serra do Mar and on the south by the Atlantic Ocean (Fig.1). This complex orographic structure and differences in surface temperatures define the local air mass circulation system and influence the dispersion of air pollutants in the Cubatão region through sea breezes, slope and valley winds, plains and plateau winds. Annual rainfall was 3330 mm from 1937 to 2007, and the wet season lasts from December to March (rainfall> 300 mm month-1) while dry season, from June to August (rainfall < 150 mm month-1) (Vieira-Filho 2015). Historical data from the Henry Borden rainfall station recorded a high annual rainfall of 2953 mm (average of 53 years) (IPEN 1986).

Meteorological and air quality studies indicate the existence of two aerial basins: the center of Cubatão and an outlying district called Vila Parisi. The central part is dominated by gaseous emissions resulting from burning of petroleum and its derivatives. On the other hand, fertilizer, steel and cement complexes are common in Vila Parisi (Abbas et al. 1993). In general, these fluvial sediments are apt to anthropogenic pertubations to various extents, including waste drainage from domestic and industrial sources, especially the phosphogypsum waste deposits in the hydrographic basin of the Mogi River (Fig. 2). Phosphogypsum is a waste by-product of the phosphate fertilizer industry, and the two main producers in the area use an igneous phosphate rock from carbonatite complexes as raw material. The major problem of using this material is the relatively high levels of natural uranium and thorium decay series and other elemental impurities (Santos et al. 2002).

2.1. Geological setting

2.1.1. Crystalline rocks

The study area is located in the Ribeira Belt, SE Brazil, which corresponds to the central portion of the Mantiqueira Province. This region is defined as superposition of orogenic systems that resulted from the collision between the São Francisco Plate, the Rio de La Plata Craton and the Luíz Alves Cratonic Fragment (Heilbron et al. 2008).

Two distinct major tectonostratigraphic terranes can be divided in the study area, separated by the large NE-SW trending Cubatão fault zone (Silva et al. 1977; Chieregati et al. 1991): the *Embu* and *Costeiro* complexes (Fig. 1). Both of these terranes were intruded by large volumes of Neoproterozoic granites, spanning a wide age interval of 150 Ma (~650-500 Ma) (Alves et al. 2013).

The *Costeiro Complex* is predominantly composed of high-grade granite-granodiorite gneisses and migmatites. In the southern portion, augen-gneiss rocks with frequent intercalations of granitic bands and amphibolite lenses are the predominant rock types (Hasui et al. 1981). High-grade metasedimentary rocks comprise sillimanite-biotite schists, quartzites and (sillimanite)-garnet-bearing biotite gneisses, with minor occurrences of calcsilicate rocks mapped in the city of São Sebastião (Silva et al. 1977; Meira et al. 2019). Syn-tectonic granites comprise peraluminous garnet-bearing leucogranites and metaluminous hornblende-biotite-bearing granites and granodiorites (Meira et al. 2019). The *Embu Complex*, on the other hand, consists of a succession of variably metapelitic rocks, biotite-quartz schists, garnet-biotite schists, phyllites, paragneisses, as well as minor calcsilicate rocks with quartzite intercalations and orthogneisses (Silva et al. 1977; Chieregati et al. 1991).

2.1.2. Sedimentary cover

The study presents the characterization of river channels and associated overbank sedimentation, lagoon deposits (mangrove), swamp sediments (fine sands and organic clays) and intertidal beach sediments of Holocene age (Suguio et al. 1978; Chieregati et al. 1991). The most recent and alluvial sediments are undifferentiated and can cover the marine and lagoon formations. Several dating experiments were carried out on shells and wood fragments from uplifted lagoon formations to detect sea-level changes for this area; the maximum level of 5100 years B.P. seems to have been situated at + 4.6 m and that of 3500 years B.P., at + 4.0 m. About 2000 years B.P. the level may have been between 1.5 and 2.0 m above present (Suguio et al. 1978).

3. Methods

3.1.Sampling and analytical methods

Fluvial sediment samples were collected after summertime (March 2005) in the five main tributaries of the Santos-São Vicente estuarine system: Cubatão River (catchment area=83.5 km^2); Pereque River (22 km^2); Piaçaguera and Mogi rivers (65.3 km^2) and Jurubatuba River (56 km^2) (Fig.1).

The samples were collected from 0.5 m thick vertical cores on the margins of the channel, from the top until 0.5 m depth, with regular intervals (10 cm). In the Mogi River, three stations were sampled downstream (P3), in middle course (PC) and upstream of the river (PB), positioned by the point of entry of effluents from the fertilizer companies. The granite-weathering profile, including organic soil (Fig. 2E), residual soil (Fig. 2F) and saprolite rock (Fig. 2G), was collected in the upstream of the Mogi River (PB). In the Mogi upstream, the fluvial sediments represent deposits of sandy material on bars in the channel (Fig. 2A). The sediment samples of the Piaçaguera and Jurubatuba rivers were collected in regions with a mix of fresh and seawater (deposits in swamps and mangroves), where sediment are supplied to the estuary is from both river and marine sources, and the transport and deposit of this sediment are a combination of river and wave/tidal processes (Fig. 2B and C). The potential sources of rocks (geologic substrate) were sampled in each study catchment area (n=12).

A huge pile of industrial waste was found in the watershed of the Mogi and Piaçaguera rivers (Fig. 2D). Phosphogypsum waste samples were obtained from the Polytechnic School of the University of São Paulo, which made analyses of phosphogypsum from Cubatão; however, the industries remained unidentified owing to the need for confidentiality. Carbonatite rock was collected in the Cajati Mine. The sediment samples were dried at 40°C and then homogenized, sieved to retain the <0.5 mm fraction and ground to -200 mesh (0.075 mm) size in an agate mill for geochemical XRF and XRD mineralogical analysis. The rock samples and phosphogypsum waste were crushed for geochemical X-ray fluorescence spectrometric analysis.

Homogenized sediment samples were analyzed for major and trace elements on an X-ray fluorescence spectrometer (XRF-Phillips PW2400) at the Chemical Laboratory of the Institute of Geosciences of the University of São Paulo - IGC-USP, which provides routine analysis of trace elements (pressed pellet), major and minor elements (fused pellet) and loss on ignition (LOI, 480°C). For each sediment core sample, a duplicate laboratory analysis was performed to assess analytical variance (Table 3).

An aliquot of surface sediments of the vertical cores in the Cubatão, Mogi (upstream and downstream), Piaçaguera and Jurubatuba rivers was pulverized and made into pressed powder pellets for X-Ray Diffraction analysis (XRD). Mineral identification was performed using XRD and by petrographic examination of thin sections of heavy minerals, which were separated using bromoform. Differences in metal concentrations between certified values and values found in this study were usually <10%. Precision and accuracy of major and trace element determination were monitored by the analysis of JG-1a reference material (Table 1).

3.2. Classification and assessment of sediment contamination

Feldspars are by far the most abundant of the reactive (labile) minerals; consequently, the dominant process during chemical weathering is the degradation of feldspars and concomitant formation of clay minerals (McLennan et al. 1993). Calcium, sodium and potassium are usually removed from feldspars by aggressive soil solutions; therefore, the proportion of alumina to alkalis typically increases in the weathered product. A good measure of the degree of weathering can be determined by calculation of the chemical index of alteration (CIA), proposed by Nesbitt and Young (1982), using molecular proportions: CIA= $[Al_2O_3/(Al_2O_3+CaO^*+Na_2O+K_2O) * 100]$, where CaO* represents the amount in silicates only. In this study, CaO was corrected if the remaining number of moles was less than that of Na_2O contents; thus, this CaO value was adopted. If the number of moles was greater than Na_2O, CaO* was assumed to be equivalent to Na_2O (McLennan et al. 1993). The CIA values of about 45-55 indicate that there was virtually no

Table 1 – Analysis of JG 1a reference material.

	JG 1a			
	Certification	**This work**	**Recovering %**	**Limit of detection**
%				
SiO_2	72.19	72.68	100.68	0.03
Al_2O_3	14.22	14.31	100.63	0.01
MnO	0.06	0.06	100.00	0.002
MgO	0.69	0.65	94.20	0.01
CaO	2.13	2.14	100.47	0.01
Na_2O	3.41	3.29	96.48	0.02
K_2O	4.01	3.96	98.75	0.01
TiO_2	0.25	0.243	97.20	0.007
P_2O_5	0.08	0.091	113.75	0.003
Fe_2O_3	2.05	2.03	99.02	0.01
LOI	0.59	0.59	100.00	0.01
Total	99.68	100.04		
ppm				
Ba	458	468	102.18	37
Ce	45.2	39	86.28	35
Cl		394		50
Co	5.7	6	105.26	6
Cr	18.6	29	155.91	13
Cu	1.3	<5		5
F	450	637	141.56	550
Ga	17	17	100.00	9
La	21.8	<28		28
Nb	12	14	116.67	9
Nd	21	<14		14
Ni	6.4	8	125.00	5
Pb	27	25	92.59	4
Rb	180	182	101.11	3
S	10	<300		300
Sc	6.31	<14		14
Sr	185	186	100.54	2
Th	12.1	10	82.64	7
U	4.7	3	63.83	3
V	23	21	91.30	9
Y	31.6	35	110.76	2
Zn	38.8	39	100.52	2
Zr	121	123	101.65	2

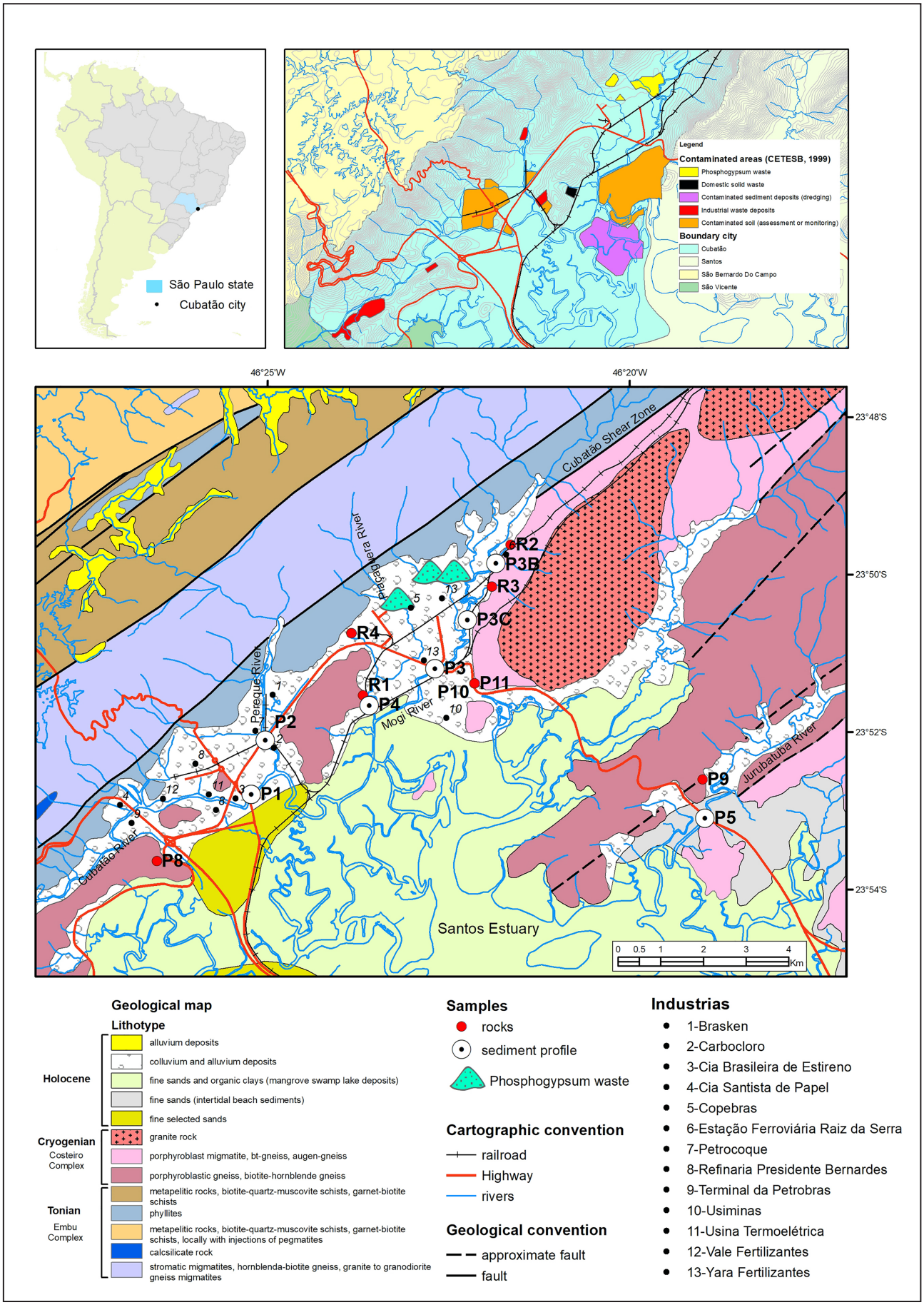

FIGURE 1. Geological map of the study area with location of samples (adapted from Chieregati et al. 1991).

FIGURE 2. A: Deposits of coarse sediments on bars in the channel of Mogi upstream River; B: Deposits in the mudflats of the Piaçaguera River; C: Google Earth view of deposits in the mangrove of the Jurubatuba River; D: View of the giant pile of industrial waste deposited in the watershed of the Mogi River (phosphogypsum); E: Detail of organic soil and gastropod shells and pellets found during sieving; F: Detail of residual soil; and G: Detail of saprolite granitic rock.

weathering (the average upper crust has a CIA value of about 47), whereas values of 100 indicate intense weathering with complete removal of the alkali and alkaline earth elements. The calculated CIA values are shown in Table 3.

A comparison of the chemical concentrations of the samples with the usual sandstone classifications, applicable for terrigenous sands and shales, is shown in the diagram for SiO_2/Al_2O_3 vs. Fe_2O_3/K_2O, as proposed by Herron (1988) (Fig. 3A).

A quantitative measure of metal pollution in aquatic sediments has been introduced by Müller (1969), and it is called the "Index of Geoaccumulation" (Igeo). The Igeo can be used to determine the heavy metal pollution status in fluvial sediments by comparing differences between the site concentration of a given metal and the geochemical background (e.g. Förstner et al. 1990; Modak et al. 1992; Rodrigues Filho and Maddock 1997; Varol 2011; Wei et al. 2011; Gao and Li 2012; Okbah et al. 2014; Kim et al. 2018) using the equation: $Igeo = \log_2(C_n/1.5*B_n)$; where C_n is the concentration of the trace element examined in the sediment samples, and Bn is the geochemical background concentration of the metal (n). Owing to lithological variability, the value of 1.5 is used the background matrix correction factor.

In this study, the background values were based on the mean value of rock samples analyzed in the study area. The Igeo defines seven classes of sediment quality to assess the degree of metal pollution. Class 0 (practically unpolluted): Igeo<0; Class 1 (unpolluted to moderately polluted): 0<Igeo<1; Class 2 (moderately polluted): 1<Igeo<2; Class 3 (moderately to heavily polluted): 2<Igeo<3; Class 4 (heavily polluted): 3<Igeo<4; Class 5 (heavily to extremely polluted): 4<Igeo<5; Class 6 (extremely polluted): Igeo>5. The highest grade (e.g., Igeo=6) reflects 100-fold enrichment above the background value.

In addition, the element concentrations were normalized to the standard concentration of elements in the upper continental

crust (UCC; Taylor and McLennan 1985; Wedepohl 1995) for a continental scale analysis. Also for a regional scale analysis, the use of confidence and prediction interval of robust linear regression method are important tools for establishing a regional history and assessing the enrichment of metal traces, as described in previous studies (Schropp et al. 1990; Grant and Middleton 1998; Kim 2016; Kim et al. 2017).

3.3. Robust linear regression

Robust Regression Analysis is used for its ability to detect outliers (Rousseeuw and Leroy 1987; Maronna et al. 2019), without subjective decisions to exclude individual samples from the regression calculations, as recommended in least square statistical methods (e.g., Luoma 1990; Grant and Middleton 1998; Kim et al. 2017). The function computes an MM-type regression estimator (Yohai 1987; Yohai et al. 1991), which may be more powerful and less subjective than least-square regression. The computation is carried out by the RStudio software. Regression analysis is used to remove the dependency of concentrations on grain size, caused by variations in sediment texture (Grant and Middleton 1998).

3.4. Principal component analysis

Principal Component Analysis (PCA) was applied as an exploratory tool to examine and identify the main interrelation among the elemental variables. The central idea of principal component analysis is to reduce the dimensionality of a data set consisting of a large number of interrelated variables. This is achieved by transforming them into a new set of variables, the principal components (PCs), which are uncorrelated, and which are ordered so that the first few retain most of the variation present in all of the original variables. For each PC, there is a coefficient or loading for each variable, and because variables are geographical locations, each loading can be plotted on a map to aid interpretation (Jolliffe 2002). The computation is carried out by the RStudio software.

A selection of the most correlated variables of the dataset was validated with the Kaiser-Meyer-Olkin (KMO) index (Kaiser 1974), which introduced the Measure of Sampling Adequacy (MSA) of factor analytic data matrices. Kaiser (1974) suggested that MSA> 0.5 is acceptable for this analysis.

Centered log-ratio transformation was performed to remove the effects of closure in a data matrix. Most analytical chemical data for major, minor and trace elements have a closed form, i.e. for a physical individual sample, they sum to a constant, whether it be percent, ppm (mg/kg), or some other units. As a result, as some elements increase in concentration, others must decrease, which leads to correlation measures and graphical presentations that do not reflect the true underlying relationships. A centered log-ratio is a procedure used for removing closure effects (Aitchison 1986). Principal component analysis was applied to infer the source of trace metals (natural or anthropogenic) and the study of interrelationships among the major and trace elements in the fluvial sediments.

4. Results and discussion

The sediment core samples are characterized by textures ranging from sandy to silty-clay sized particles, poorly selected with angular grain shape. In the Mogi River basin, the sediment showed medium to coarse-grained sands in the upstream (bar deposits) and middle course, and higher clay and silt contents in the downstream zone, with organic clays in the Piaçaguera River (Table 2).

Table 3 shows the major and trace elements analyses of the sediment cores, potential source rocks (n=12), weathering profile (organic soil, residual soil and saprolite rock), phosphogypsum waste and carbonatite ore samples.

The minerals in the fluvial sediments include quartz, K-feldspars and plagioclase as major phases, biotite, hornblende, garnet, magnetite, epidote, zircon, monazite, apatite, tourmaline and aluminous-silicate, as minor phases. The clay minerals identified by X-ray diffraction are predominantly kaolinite, gibbsite, montmorillonite, muscovite and chlorite (Table 1).

Table 2 – Field description and x-ray diffractometric results.

River	Field description	X-ray diffractometry
Cubatão (P1)	Fine sands, sand-silt texture, brown color, dark gray plane-parallel bedding, poorly-sorted sediments	Quartz – SiO_2; Muscovite – (rich V-Ba) $(K,Ba,Na)_{0.75}(Al,Mg,Cr,V)_2(Si,Al,V)_4O_{10}(OH, O)_2$; Mica rich in Fe – $(Mg, Fe)_6(Si, Al)_4O_{10}(OH)8$; Kaolinite - $Al_2(Si_2O_5)(OH)_4$; Gibbsite - $Al(OH)_3$
Pereque (P2)	Medium to fine sand and brown color up to 23cm, fine sand, silt-clay texture, dark gray and organic matter	Not measured
Mogi River upstream (P3B)	Medium to coarse-grained sand with quartz, muscovite, feldspar, poorly-sorted and lithic fragments	Quartz – SiO_2; Muscovite $KAl_2(AlSi_3O_{10})(OH)_2$; Kaolinite - $Al_2(Si_2O_5)(OH)_4$; Montmorillonite – $(Na,Ca)_{0.3}(Al, Mg)_2Si_4O_{16}(OH)_2xH_2O$
Mogi River middle (P3C)	Medium to fine sand, silt-clay texture	Not measured
Mogi River downstream (P3)	0-20cm: Fine and medium sand, silt-sand texture, poorly-sorted; 20-50cm: fine sand, silt-clay texture and organic matter	Quartz – SiO_2; Muscovite – (rich V-Ba) $(K,Ba,Na)_{0.75}(Al,Mg,Cr,V)_2(Si,Al,V)_4O_{10}(OH, O)_2$; Gibbsite - $Al(OH)_3$; Feldspar (microclinic) – $(K_{.95}Na_{.05})AlSi_3O_8$
Piaçaguera River (PA)	Fine-grained muddy sediments, dark gray clay and rich in organic matter	Chlorite - $(Ni, Mg, Al)_6(Si, Al)_4O_{10}(OH)_8$ Muscovite - (rich V-Ba) $(K,Ba,Na)_{0.75}(Al,Mg,Cr,V)_2(Si,Al,V)_4O_{10}(OH, O)_2$
Jurubatuba River (P5)	Fine to medium sand, poorly-sorted, gray color and homogeneous	Quartz – SiO_2; Muscovite – (rich V-Ba) $(K,Ba,Na)_{0.75}(Al,Mg,Cr,V)_2(Si,Al,V)_4O_{10}(OH, O)_2$; Montmorillonite – $(Na,Ca)_{0.3}(Al, Mg)_2Si_4O_{16}(OH)_2xH_2O$; Gibbsite - $Al(OH)_3$; Feldspar (microclinic) – $(K_{.95}Na_{.05})AlSi_3O_8$
Organic Soil	Black color, sand-silt texture and organic matter; was found (i) Fe-pellets from steel plants due to the proximity of train tracks carrying iron ore; (ii) Gastropod shell	Quartz – SiO_2; Muscovite – (rich V-Ba) $(K,Ba,Na)_{0.75}(Al,Mg,Cr,V)_4°_{10}(OH, O)_2$; Kaolinite – $Al_2(Si_2O_5)(OH)_4$; Gibbsite – $Al(OH)_3$; Goethita – FeO(OH); Feldspar (microclinic) – $(K_{.95}Na_{.05})AlSi_3O_8$;
Residual Soil	Silt-sand texture, yellow-orange colors, abundant quartz and feldspars and organic matter.	Not measured

Table 3 - Major and trace elements of vertical profile in sediment samples of the upper portion of Santos estuarine system.

Local	Depth	SiO_2	Al_2O_3	MnO	MgO	CaO	Na_2O	K_2O	TiO_2	P_2O_5	Fe_2O_3	LOI	CIA	Ba	Ce	Cl	Co	Cr	Cu	F	Ga	La	Nb	Nd	Ni	Pb	Rb	Sc	Sr	Th	U	V	Y	Zn	Zr	S
	(cm)	%												ppm																							
P1 Cubatão	0-5	58.54	16.94	0.111	1.77	0.54	0.42	2.77	0.929	0.162	7.22	9.08	79.5	647	101	349	22	85	40	1047	24	46	18	38	39	36	130	12	81	15	9	99	34	138	351	328
	5-10	61.33	15.86	0.134	1.61	0.51	0.38	2.61	0.895	0.137	6.99	7.91	79.6	584	90	416	26	78	39	1052	23	43	17	44	35	44	121	13	73.6	14	9	90	32	114	364	<LD
	5-10	70.69	11.37	0.06	1.23	0.77	0.47	2.67	0.614	0.504	4.37	5.94		632	100	412	46	80	36	1651	20	46	17	44	33	44	121	16	75.8	6	5	102	33	105	367	<LD
	10-20	64.15	14.86	0.126	1.51	0.45	0.34	2.52	0.847	0.136	6.35	7.06	79.4	577	93	291	36	76	36	986	21	38	18	50	34	33	116	11	87	13	8	90	31	106	337	<LD
	40-50	67.69	13.57	0.119	1.29	0.34	0.24	2.27	0.741	0.114	5.44	6.42	80.7	504	83	386	30	79	38	811	20	43	16	40	34	43	100	12	52.6	10	8	80	27	99	310	307
P2 Pereque	0-5	81.45	7.15	0.038	0.96	0.23	0.17	1.32	0.55	0.054	3.57	3.37	78.2	296	56	<LD	43	59	19	1168	13	28	13	40	21	11	62	7	27.3	2	6	57	21	70	215	<LD
	5-10	79.12	8.24	0.041	1.1	0.24	0.17	1.47	0.612	0.049	4	3.4	79.3	303	70	261	12	56	20	834	12	34	10	44	23	23	64	5	26.5	9	7	57	23	77	230	<LD
	10-20	77.09	8.96	0.042	1.09	0.26	0.2	1.53	0.64	0.065	4.07	4.64		325	70	<LD	42	57	23	838	14	33	16	26	25	17	70	7	33	6	7	62	24	85	243	559
	10-20	77.56	8.95	0.04	1.06	0.27	0.19	1.54	0.638	0.066	4.08	4.66	79.5	335	58	<LD	43	60	26	841	14	39	16	42	25	16	69	7	32.6	6	7	65	23	85	242	556
	40-50	66.06	13.2	0.052	1.29	0.44	0.18	1.82	0.879	0.134	5.52	9.19	83.7	417	100	178	48	77	32	855	19	42	22	46	34	36	79	12	44.2	12	8	96	30	97	353	6220
P3 Mogi downs-tream	0-5	64.77	13.66	0.082	1.39	0.86	0.41	2.6	0.822	0.548	5.62	7.01	76.6	917	589	<LD	131	57	32	3352	21	285	62	291	26	27	142	12	387.3	27	8	71	46	100	405	753
	5-10	66.38	13.66	0.062	1.47	0.75	0.47	2.87	0.743	0.348	5.26	6.63	74.6	869	519	194	25	53	28	3139	21	256	45	235	27	40	158	11	432.5	25	7	66	38	92	284	861
	10-20	72	10.9	0.057	1.22	0.66	0.47	2.66	0.611	0.3	4.12	5.41	71.1	474	164	53	128	53	24	1734	17	80	33	82	20	26	148	7	96.2	14	7	53	27	87	304	505
	40-50	69.87	11.4	0.06	1.24	0.77	0.43	2.65	0.61	0.496	4.37	5.94	71.9	513	168	269	24	53	27	1847	18	71	23	78	22	44	149	8	104.7	15	8	55	29	111	305	446
	40-50	70.69	11.37	0.06	1.23	0.77	0.47	2.67	0.614	0.504	4.37	5.94	72.7	506	167	245	25	52	26	1500	18	79	22	73	23	42	147	10	104.3	14	8	54	28	113	305	452
PB Mogi upstream	0-10	75.95	11.57	0.049	0.64	0.22	0.69	4.93	0.367	0.052	2.74	2.09	60.3	578	<LD	78	25	31	14	846	16	<LD	14	<LD	14	38	212	<LD	69.3	11	<LD	40	15	49	128	<LD
	10-20	83.31	7.41	0.04	0.68	0.3	0.42	2.71	0.442	0.049	2.41	1.75	63.2	331	68	<LD	48	27	13	519	10	34	19	17	12	19	130	<LD	40.6	14	<LD	34	23	42	198	<LD
	20-30	77.01	9.97	0.091	0.84	0.37	0.47	3.23	0.804	0.069	4.19	2.17	66.4	474	100	<LD	46	46	18	885	15	48	25	55	16	20	145	<LD	44.7	30	<LD	63	42	55	362	<LD
	20-30	77.03	10.01	0.091	0.84	0.37	0.46	3.23	0.81	0.068	4.2	2.22		464	95	<LD	46	46	17	730	14	58	24	60	14	20	145	<LD	44.9	30	<LD	58	42	56	362	<LD
PC Mogi middle	0-10	80.26	8.42	0.049	1.05	0.48	0.46	2.34	0.497	0.066	3.04	2.76	67.5	299	52	<LD	12	39	14	831	12	<LD	14	24	16	18	129	<LD	39.4	13	<LD	41	25	51	261	<LD
	10-20	80.11	8.35	0.045	1.05	0.45	0.35	2.2	0.479	0.067	3.11	3.2	70.3	306	50	<LD	68	36	17	977	11	<LD	23	26	18	16	121	<LD	37.8	11	<LD	43	23	56	251	<LD
	20-30	71.91	11.79	0.065	1.48	0.52	0.39	2.62	0.645	0.099	4.51	5.56	74.1	393	47	<LD	66	51	24	1311	17	33	25	43	24	23	145	<LD	41.6	14	<LD	70	30	74	325	<LD
	20-30	71.82	11.82	0.064	1.48	0.52	0.41	2.63	0.648	0.101	4.52	5.66		386	63	<LD	67	49	23	1172	17	34	25	40	25	25	145	<LD	42.1	15	<LD	63	29	74	326	<LD
	30-40	72.98	11.44	0.068	1.48	0.56	0.53	2.6	0.619	0.096	4.47	5.12	71.5	412	74	<LD	31	53	22	958	17	40.3	19	42	24	24	146	<LD	43.4	16	<LD	56	29	72	318	<LD
	40-50	74.28	11.13	0.059	1.3	0.47	0.48	2.63	0.605	0.094	4.23	4.4	71.5	388	57	<LD	51	62	22	1214	16	30	23	32	22	21	143	<LD	42.8	12	<LD	56	27	70	301	<LD
PA Piaçaguera	0-10	30.79	27.88	0.036	0.46	0.24	0.34	1.03	1.151	0.997	9.92	24.02	92.6	287	136	786	21	93	32	1540	46	63	30	105	39.6	56	55	16.7	77	22	6	181	18	109	107	5013
	10-20	36.81	22.84	0.061	1.17	0.69	0.86	1.82	1.017	1.011	9.34	25.04	82.6	515	138	3564	35	176	46	2397	34	94	27	140	48.2	72	105	16	117.5	22	28	157	66	167	153	18648
	20-30	38.55	25.23	0.149	1.02	0.32	0.5	1.67	1.139	1.194	10.48	20.54	88.0	404	197	1977	23	93	44	1914	40	78	25	113	37.8	73	81	16	58.4	22	18	170	79	110	202	4086
	20-30	38.42	25.01	0.146	1	0.32	0.54	1.68	1.136	1.235	10.5	20.37		403	166	2028	24	93	43	1981	39	85	25	102	37.4	73	80	17	57.6	23	19	158	78	113	201	4166
	30-40	52.45	20.68	0.048	0.91	0.3	0.46	1.64	1.003	0.228	5.69	17.03	86.3	331	107	1345	27	59	37	1373	30	39	21	60	29.1	62	86	<LD	64.9	15	<LD	120	29	127	280	5690
	40-50	54.59	15.28	0.048	1.13	0.45	0.7	1.61	0.828	0.122	5.09	20.56	79.1	308	87	1772	39	56	25	1122	21	42	19	42	22	46	79	<LD	82	9	<LD	91	28	99	222	22618
Jurubatuba	0-5	62.27	12.84	0.046	1.64	1.24	1.63	3.12	0.645	0.143	3.69	6.63	59.5	574	55	2377	96	73	20	1130	19	24	21	<LD	19	40	131	8	174.2	7	8	68	15	72	306	3110
	5-10	64.65	13.22	0.045	1.66	1.18	1.54	3	0.659	0.161	3.87	7.88		550	75	2260	72	71	12	821	21	36	23	32	20	46	130	8	171.6	7	8	68	16	74	296	3293
	5-10	64.81	13.32	0.045	1.64	1.18	1.54	3.01	0.665	0.159	3.88	7.94	61.4	550	66	2174	70	74	13	806	18	29	23	24	23	44	131	9	172.7	8	8	69	17	72	296	3318
	10-20	66.2	12.65	0.044	1.57	1.18	1.51	2.92	0.646	0.143	3.67	7.36	60.9	515	62	1853	85	71	12	1236	18	33	23	30	20	37	122	8	163.9	8	9	67	15	69	278	4783
	40-50	58.77	15.48	0.052	1.99	1.17	1.69	3.19	0.779	0.156	4.51	10.62	63.2	584	68	2556	49	81	14	1194	22	40	19	38	26	49	142	11	173.2	11	9	86	19	89	316	8517
R3A	Rock	60.38	17.29	0.094	2.58	2.7	2.21	2.27	1.209	0.366	7.14	2.62	70.7	852	109	<LD	58	<LD	<LD	1544	27	46	16	54	19	12	163	<LD	498.2	11	6	145	15	113	185	<LD
P8B		67.74	14.06	0.082	1.37	3.04	2.93	4.13	0.522	0.176	3.69	0.9	58.2	1296	102	19.5	17	17	9	731	13	56	16	35	14	22	151	12	412.4	12	5	57	31	52	165	<LD
P11A		68.05	15.3	0.042	0.87	2.32	2.89	5.33	0.602	0.185	3	0.33	59.2	1199	111	<LD	51	<LD	10	1013	19	48	25	30	<LD	47	202	<LD	338.8	18	3	50	23	55	191	<LD
P 1		68.55	16.38	0.044	1.05	3.19	3.7	1.2	0.295	0.1	2.76	1.6	66.7	427	<LD	<LD	48	<LD	6	1992	20	<LD	10	<LD	9	13	128	<LD	480.4	7	5	37	3	51	102	<LD
R1		69.18	16.11	0.028	0.63	1.46	2.77	4.78	0.386	0.118	2.26	1.5	64.1	333	<LD	<LD	50	<LD	6	<LD	27	<LD	14	14	<LD	30	90	<LD	278.4	13	16	25	9	50	125	<LD
R2		69.58	16.93	0.028	0.79	2.02	4.46	1.44	0.313	0.05	2.26	1.39	68.1	852	49	25	78	<LD	2.5	564	21	<LD	20	1	5	28	166	<LD	364.9	<LD	<LD	39	12	46	153	<LD
R3B		70.65	15.23	0.023	0.5	0.3	1.05	6.63	0.537	0.25	2.49	1.93	65.6	489	155	441	52	<LD	5	1458	23	83	23	78	<LD	56	295	<LD	79	61	<LD	17	18	56	283	<LD
P9		72.27	14.41	0.022	0.37	1.01	2.06	5.95	0.274	0.062	1.81	1.3	61.5	1426	69	19.5	47	24	5	<LD	14	21	10	<LD	5	42	170	4	368.3	25	6	23	9	27	154	<LD
P11B		73.91	13.81	0.017	0.14	1.69	2.8	5.32	0.124	0.033	1.3	0.39	58.5	991	156	<LD	50	<LD	<LD	<LD	15	80	14	45	<LD	35	176	<LD	338.3	25	7	10	13	21	123	<LD
P10		74.24	13.29	0.021	0.13	0.68	3.36	5.24	0.115	0.03	1.23	0.39	58.9	342	136	174	72	10	2	857	17	70	30	38	<LD	54	269	4	132.5	42	8	5	37	24	138	<LD
R4		74.62	12.87	0.049	1.3	1.09	1.1	2.73	0.49	0.035	4.07	1.4	72.4	646	34	<LD	74	55	18	<LD	15	33	20	24	26	16	110	<LD	117.4	11	<LD	68	11	50	246	<LD
P8A		74.93	13.51	0.028	0.11	0.65	3.54	4.74	0.062	0.204	0.81	0.49	60.2	1329	106	188	36	20	6	1180	12	51	16	<LD	10	31	154	11	407.6	<LD	<LD	60	31	44	172	<LD
Saprolite	Soil	66.5	16.67	0.033	0.44	0.02	0.33	5.58	0.537	0.19	3.61	5.74	73.8	665	359	<LD	47	<LD	<LD	790	24.9	112	23	73	5	54	211	<LD	79.2	66	<LD	23	20	59	450	395
Residual soil		70.1	14.15	0.027	0.27	0.02	0.21	1.66	0.811	0.09	4.7	8.01	88.2	263	42	<LD	12	28	18	1376	23	<LD	22	37	10	44	100	<LD	39	18	<LD	79	13	66	303	<LD
Organig soil		54.74	9.14	0.071	0.39	0.4	0.29	1.63	0.521	0.322	6.5	17.75	79.8	504	65	<LD	65	40	88	904	11	41	20	51	41	276	92	<LD	155.6	<LD	<LD	83	17	126	228	2165.4
Carbonatite ore	Ore	0.005	0.05	0.134	3.85	51.73	<LD	0.07	0.053	5,332	2.41	36.16		850	213	<LD	34	<LD	23	2237	<LD	126	<LD	44	9	46	<LD	37	5524.6	30	83	21	38	19	<LD	4965
Phosphogypsum 1	Waste	0.005	0.11	0.017	0.03	33.75	<LD	<LD	0.523	1,288	0.77	5.84		6104	3547	<LD	<LD	<LD	9	4744	<LD	1969	171	806	11	30	<LD	17	5205.4	69	71	<LD	101	32	219	354969
Phosphogypsum 2		0.005	0.12	0.004	0.02	36.04	0.02	<LD	0.177	0.603	0.25	5.6		1351	2980	<LD	<LD	<LD	6	8987	<LD	1637	110	737	11	31	<LD	19	6179.1	81	87	<LD	100	27	263	374195

LD: limit of detection

4.1. Major and trace elements

4.1.1. Classification, weathering and sedimentary sorting

Geology provenance, weathering and erosion processes control the mineralogy and geochemical composition of fluvial sediments (McLennan 1993). In addition, hydrodynamic sorting segregates detrital minerals according to their size, shape, and density; thus, it controls mineralogy variability as well as geochemical differentiation in fluvial sediments (Garzanti et al. 2011). The upper estuarine fluvial sediments flow in the single channel to a lake margin, where an estuary was formed and any sediment introduced by the rivers is reworked and carried away by processes such as waves and tides (Nichols 2009).

In the Herron SandClass diagram, terrigenous sands and shales are classified by their SiO_2/Al_2O_3 ratios; Si-rich quartz sands are separat from Al-rich shales. The ratio of total iron (as Fe_2O_3)/K_2O separates lithic sands (litharenites and sublitharenites) from feldspathic sands (arkoses and subarkoses), and very high Fe_2O_3/K_2O ratios indicate Fe-rich shales or Fe-rich sands depending on the silica/alumina ratio. According to this classification, the upper estuarine fluvial sediments showed a trend from arkose (Mogi upstream), wacke (Jurubatuba, Mogi downstream and Cubatão), litharenite (Mogi upstream, Mogi middle course and Pereque) and shale (Cubatão) to Fe-shale (Piaçaguera) (Fig. 3A). The upper part of the Mogi River has higher SiO_2 and lower Al_2O_3 concentrations than the lower part of this river (Fig. 3C). The higher SiO_2 content in the upper part indicates a higher quartz content, and the higher K_2O suggest that mica and K-feldspar controlled the element abundances (Fig. 3D), attested with field descriptions of the medium to coarse-grained sands with quartz, muscovite, feldspars, poorly selected and lytic fragments (Table 2).

In addition, the $Al_2O_3/(Al_2O_3+CaO^*+Na_2O+K_2O)$ (A-CN-K) diagram can be used to understand trends in chemical weathering and possible source rock composition (McLennan et al. 1993; Roy et al. 2008; Pang et al. 2018; Guo et al. 2018). The upper estuarine sediments fall in the delimited field of suspended sediments from major rivers throughout the world, representing a variety of climatic regimes (Fig. 3B). The exception is the upstream sediments of the Mogi River, which are enriched in K-feldspars, biotite and muscovite, but depleted of calcium and sodium and, thus, they are plotted in the same area of the source rocks (Fig. 3 B and D), as in the Jurubatuba River.

The Piaçaguera river sediments, classified as shale/Fe-shale in the Herron SandClass diagram, and residual soil are inserted on the top of the A-CN-K diagram, as one final product of weathering of rocks, with lower K_2O-SiO_2 and high Al_2O_3 contents (Fig. 3 C and D). Fig. 3C shows that Si and Al concentrations exhibit a strong negative correlation, reflecting grain size contrast between samples. Coarse sediments are primarily composed of quartz sand, whereas fine sediments contain large quantities of clay minerals and, consequently, high Al concentrations. The sediments of the Piaçaguera River are rich in organic clay and muds from swamp deposits (LOI = 17-25%), with few feldspars and complex clay minerals (V-Ba-rich muscovite and chlorite, Table 2), as secondary products formed during advanced chemical weathering (CIA=79 to 93%). This also occurs in the residual soil (CIA=88%); NaO, CaO, K_2O and MgO have been lost from source rocks during hydrolysis and there was intense leaching of alkaline and earth alkaline cations owing to heavier rainfall.

The significant differences in chemical composition among the fluvial sediments may reflect differences in source rock types, degree of weathering of source rocks and physical segregation of clastic materials during transportation (Nesbitt and Young 1982; McLennan et al. 1993). The sediments from the Mogi (upstream and middle course) and Pereque rivers are classified as arkose/lithoarenites by Herron SandClass (Fig. 3A). However, the CIA values of the upstream river sediments showed lower CIA indexes (CIA = 60-66), when compared to the sediments of the Pereque river (CIA = 78-83). The upstream sediments were deposited in the channel with high-energy fresh water, which carries and deposits gravelly and sandy material with higher contents of feldspars, biotite, muscovite and lithic fragments (Fig. 3B). There is a trend in the ternary A-CN-K diagram for sediments from the upstream to downstream portion in the Mogi River, as well as an increase in the CIA index. This may account for the variation in the proportion of unaltered minerals (biotite and muscovite) in comparison to newly formed minerals (kaolinite, gibbsite, montmorillonite, Table 2).

By contrast, the sediments of the Piaçaguera are collected in region with a mix of fresh and seawater (swamps deposits), where sediment supply to the estuary is from both river and marine sources, and the transport and deposition of this sediment are a combination of river and wave/or tidal processes. The sample is composed of fine-grained muddy sediments, dark gray clay and high contents of organic matter (Table 2). The high chemical weathering alteration (CIA = 79 to 93) in this site can be accelerated by the flooding of the tides. Another plausible interpretation would be the existence of intertidal beach sediments during Holocene transgression events.

4.1.2. UCC-normalized fractionation patterns

Figure 4 is a standard plot of major and trace concentrations for regional rocks, saprolite rock, residual soil and organic soil normalized to the upper continental crust (UCC) values (Taylor and McLennan 1985; Wedepohl 1995). Regional rocks have predominantly granitic compositions, with some exceptions, such as diorite (R3A), and granodiorite (P8B and R2), and an intermediate composition of granodiorite - granite (P1). The R4 sample, characterized as garnet-muscovite-biotite gneiss, is genetically associated with metasedimentary rocks of the Embu Complex (Fig. 1). The UCC-normalized pattern of the regional rocks showed samples enriched in K, Rb, Co and Pb, and depletion in P, Mg, Ca, Fe, Mn, Ni, Cr, Cu, Ti, V and S elements. Systematic depletion in mobile elements of Mg, Ca, Sr and Na, and relatively enrichment in K, Rb, Pb, Ce, La, Nd and Th are associated with a weathering effect, as found in saprolite rock and residual soil. The organic soil showed enrichment of P, Co, Cu, Pb and S when compared to UCC. The high concentration of lead in the organic soil (276 ppm) can be due to the occurrence of pellets that were found in the soil when sieved (Fig.2E). This site is located close to the train line and station, which transports pellets to steelmakers at the Cubatão Industrial Hub (Fig. 1).

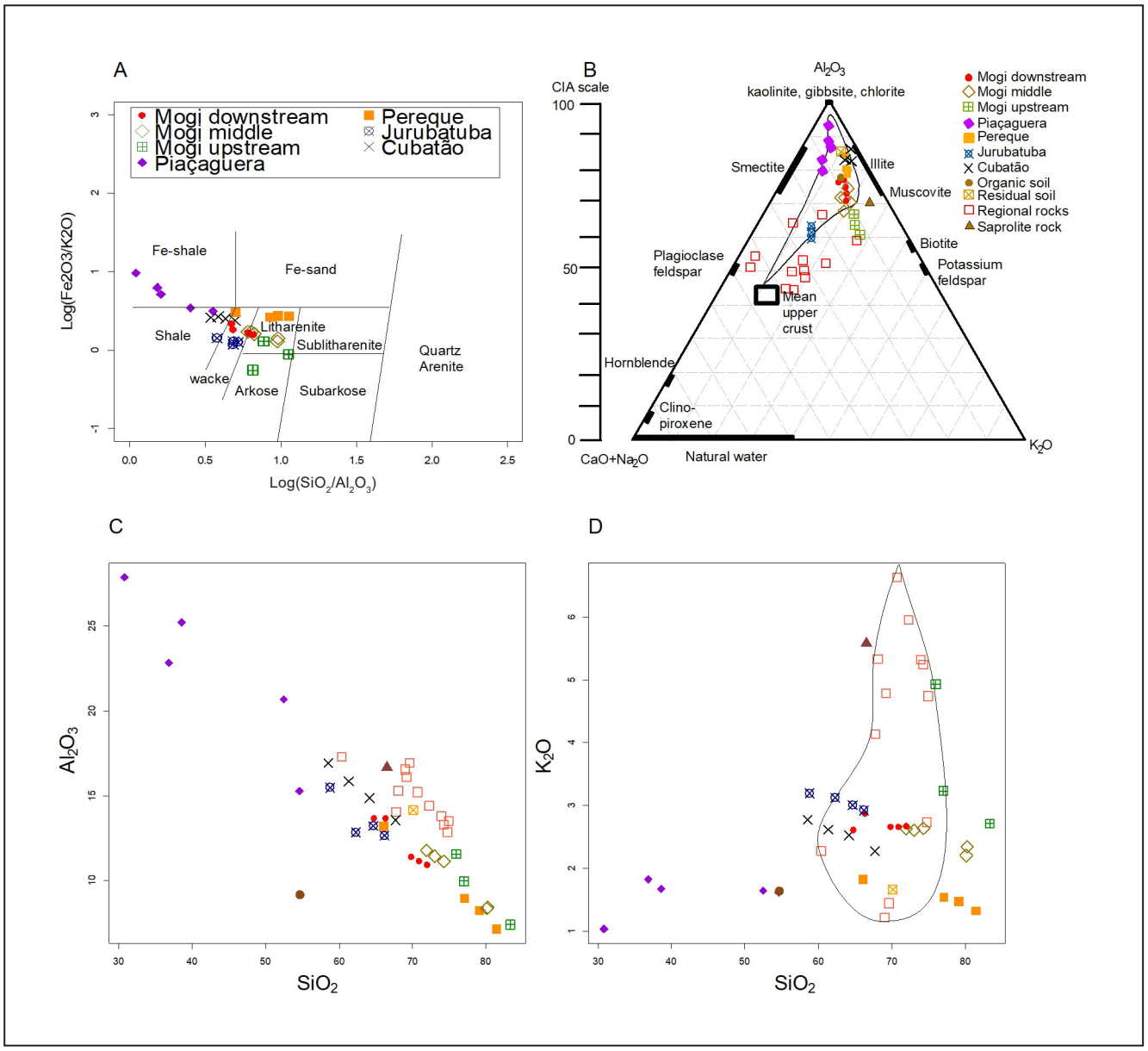

FIGURE 3. A: SandClass Geochemical classification of Herron (1988). B: A-CN-K diagram with the chemical index of alteration (CIA) scale shown on the left. Selected idealized igneous and sedimentary minerals, as well as the range of typical natural waters have also been plotted. The delimited fields are suspended sediments from major rivers throughout the world representing a variety of climatic regimes. C: Al_2O_3 vs. SiO_2 concentrations. D: K_2O vs. SiO_2 concentrations. The delimited fields are rocks from the watershed area.

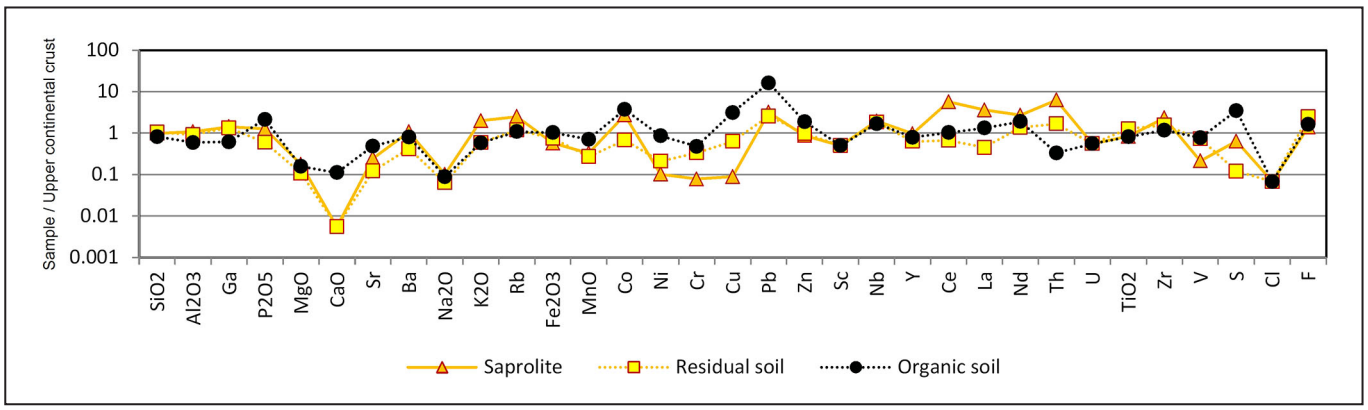

FIGURE 4. Major oxides and trace elements normalized to the standard upper continental crust (UCC) in saprolite rock, residual and organic soils collected along the upper streams of the Mogi River (multi-element diagram arranged following the periodic table group by group).

The fluvial sediment cores normalized to the upper continental crust (UCC) standard (Taylor and McLennan 1985; Wedepohl 1995) showed, in general, that Si, Ba, Rb, K, Y, Th, Ti and Zr are similar to UCC compositions, while the elements Na, Ca, Mg, Sr, Cr, Ni and Mn were depleted (Fig. 5). The sediments of the Piaçaguera and Mogi rivers are relatively enriched in P, Al, Ga, Sr, Ca, Cr, Cu, Pb, Zn, La, Ce, Nd, Y, U and F from upstream to downstream. These fluvial sediments have higher concentrations of P, Co, Ce, La, Nd, U, S, Cl and F than the other rivers (Fig.5).

4.1.3. Geo-accumulation index (Igeo)

The index of geo-accumulation (Igeo), summarized in Fig. 6, is a proxy for measuring the pollution status of sediments or identifying elemental enrichments in relation to the background (regional rock composition, Table 3). The latter is considered to be representative of the lithological composition of the local catchment.

Most of the analyzed fluvial sediments are enriched in Fe and Mn (Table 4), as well as organic matter (LOI). The iron leaves the silicate and sulfide minerals and, when oxidized by interaction with surface chemical forces, forms a new oxy-hydroxy phase (Bauer and Velde 2014). The surfaces of these minerals are similar to the edge surface sites in clays and can find various transition metals in coatings on oxides (Manceau et al. 2007). The principal factors affecting the availability of heavy metals absorbed in hydrous oxide minerals are Eh, pH, concentration of the metal of interest, concentration of competing metals, concentration of other ions capable of forming inorganic complexes, and organic chelates (Jenne 1968).

The fluvial sediments, in general, were enriched in LOI with the exception of the Mogi River upstream (LOI <2.2%). LOI enrichment occurred in the sediments of the Piaçaguera River (17-25%), and there were high levels of heavy metals in this location (Cr, Cu, Ni, Pb and Zn), classified as moderately to heavily polluted (Table 4). However, high contents of organic matter in these sediments can adsorb heavy metals. This has been deduced from a significant positive correlation of the LOI and the heavy metal contents of sediments (Table 5). The mechanism of heavy metal fixation by organic matter are presumed to cause the formation of complexes and chelates (Jenne 1968). The role of organic matter is to produce a periodic reducing environment required to maintain manganese and iron oxides under hydrous microcrystalline conditions (Jenne 1968).

The organic soil showed muscovite (rich V-Ba ($K,Ba,Na)_{0.75}(Al,Mg,Cr,V)_2(Si,Al,V)_4O_{10}(OH,O)$), kaolinite ($Al_2(Si_2O_5)(OH)_4$), gibbsite ($Al(OH)_3$), goethita ($FeO(OH)$) and feldspar microclinic ($K_{.95}Na_{.05})AlSi_3O_8$ in X-ray diffraction analysis (Table 2). The vanadium-rich muscovite may explain the significant correlation between Al-Fe-V (Table 5) in organic soils and fluvial sediments.

The elements Nd, Sc, Ti, Y and Zr also appear little enriched in fluvial sediments compared to the background, and the former can represent the natural accumulation of the resistant heavy minerals. The exception was Mogi downstream river located downstream of the areas most significantly contaminated by phosphogypsum waste (Fig. 1), which had a moderately to heavily polluted class for Ce, La and Nd (Table 4).

4.1.4. Robust Linear Regression

The influence of grain size on concentration of contaminants in sediments is well known, and apparent contamination differences between sites may reflect grain size rather than the extent of contamination; in addition, samples may be grouped together purely because of similarities in sediment texture (Grant and Middleton 1998). Thus, the baseline regression line is frequently used to remove the dependency of concentration on grain size. This may be done using concentrations of a conservative grain-size proxy element (scandium). A larger number of samples is required and, preferably, at the local, regional and continental scales. To this end, the following compilations have been made: (i) data on Cr, Cu, Ni, Pb, Sc, V and Zn of the sediments (n=257) from the Santos-São Vicente estuary (Kim 2016); (ii) three sediment-core (n= 81) in the Santos estuary (Fukumoto 2007); and (iii) data on Ce, Co, Cr, La, Nd, Rb, Sc, Th, U, Zn and Zr of the sediments from the Santos Bay (n= 9), São Vicente channel (n= 10), estuarine rivers (n= 13), Mogi river (n= 10) and a sediment core in the Mogi river (n= 16) (Silva 2004).

All of these data were then analyzed together with our samples (n=30) and the regression line and 95% confidence and prediction bands were computed by the RStudio software (Fig. 7). Among our data, the results indicated enrichment in the Cubatão (Co, Cr and Ni), Pereque (Co, Cr and Ni), Mogi upstream (Co, Pb, Rb and Th), Mogi middle (Co, Cr and Ni), Mogi downstream (Ba, Ce, Co, Cr, La, Nd and Pb), Piaçaguera (Co, Cr, Cu, Ni, Nd, Pb, U and Zn) and Jurubatuba (Co, Cr and Pb) rivers.

Cobalt is enriched in all sediment cores analyzed in the upper estuary (Fig. 7 and 8) and in comparison to the UCC composition (Fig. 5). However, the Igeo values of cobalt have not been enriched (Igeo<0), which suggests natural origin and low mobility in surface geochemistry. This also occurred with the Pb element, although locally enriched in sediment cores from Santos bay (Fukumoto 2007) and sediments from the Piaçaguera and Jurubatuba rivers (Fig. 7). The Igeo values of Pb indicate that it comes from regional rocks (predominance of granitic rocks), although the anthropogenic origin is not discarded for certain localities (e.g. organic soil).

Ba, Ce, La and Nd were found in high contents in phosphogypsum waste (Table 3). These elements are classified into moderately to heavily polluted in the downstream of the Mogi River sediment core (Table 4), and they are also enriched compared to the upper continental crust (Fig. 5). Silva (2004) also found anomalous contents of these elements, especially in the sediment core of the Mogi River (Fig. 7).

4.1.5. Principal component analysis

The results of PCA revealed three principal components (PCs) considering the eigenvalues greater than unity that explain 84.4% of the total variance for the major elements and 74.2% of the total variance for the trace elements (Table 5, Fig. 9). The PC1 for the major elements has positive loading on Fe, Al, P and Ti, which are lithophile elements commonly concentrated in residual soils and residual sediments (immobile elements) and LOI relative to organic matter. The negative loading on K, Ca, Mg, Si and Na grouped the major elements of silicate minerals that are the products of rocks and soils weathered on land. PC2 separated mobile elements (Na and Ca) from immobile elements such as Fe, Ti and Mn (Fig. 9). PC3 separated Ca and Mg from Na and K, which can

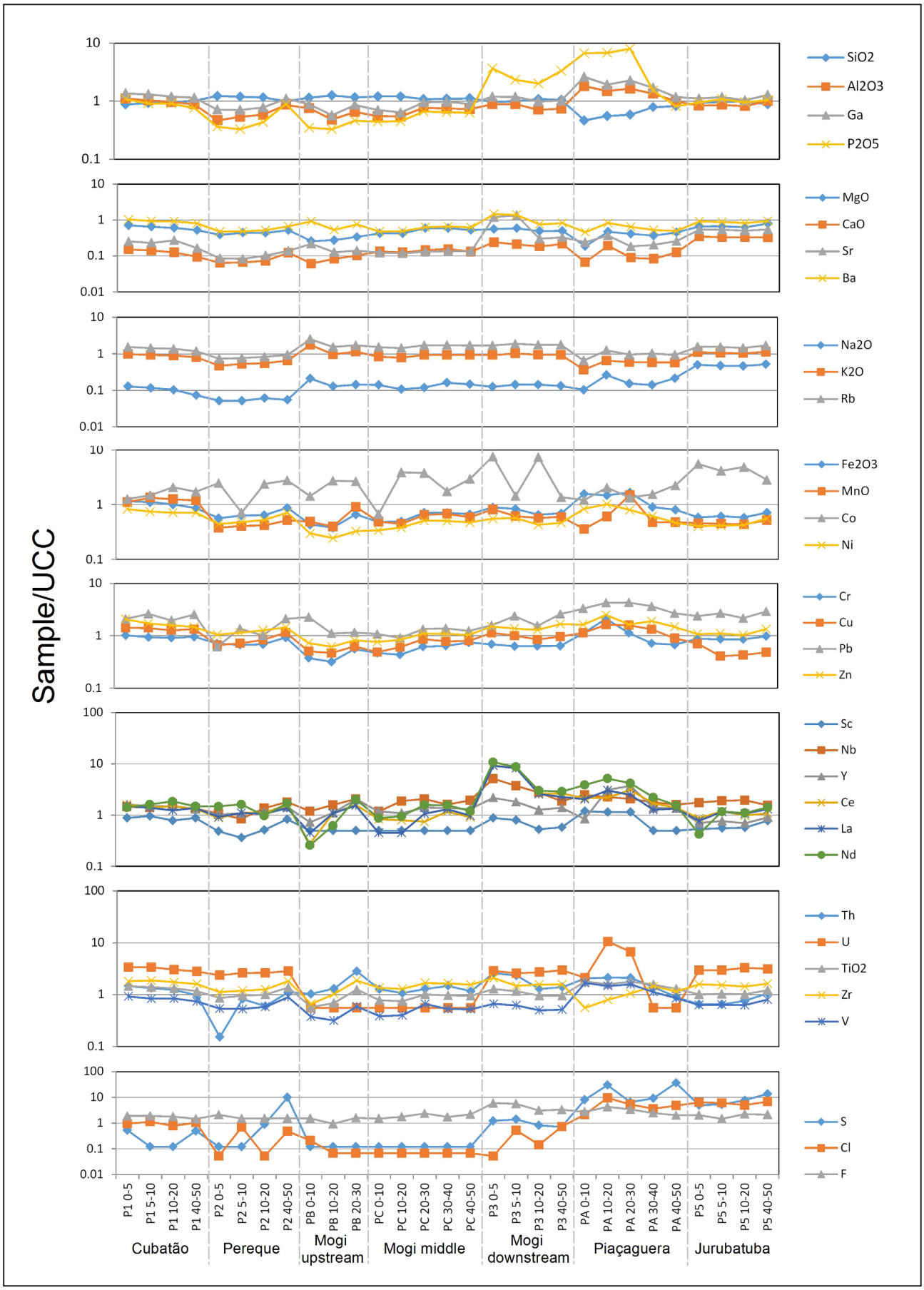

FIGURE 5. Major oxides and trace elements normalized to the standard upper continental crust (UCC) in river sediments cores collected along the upper Santos estuarine system.

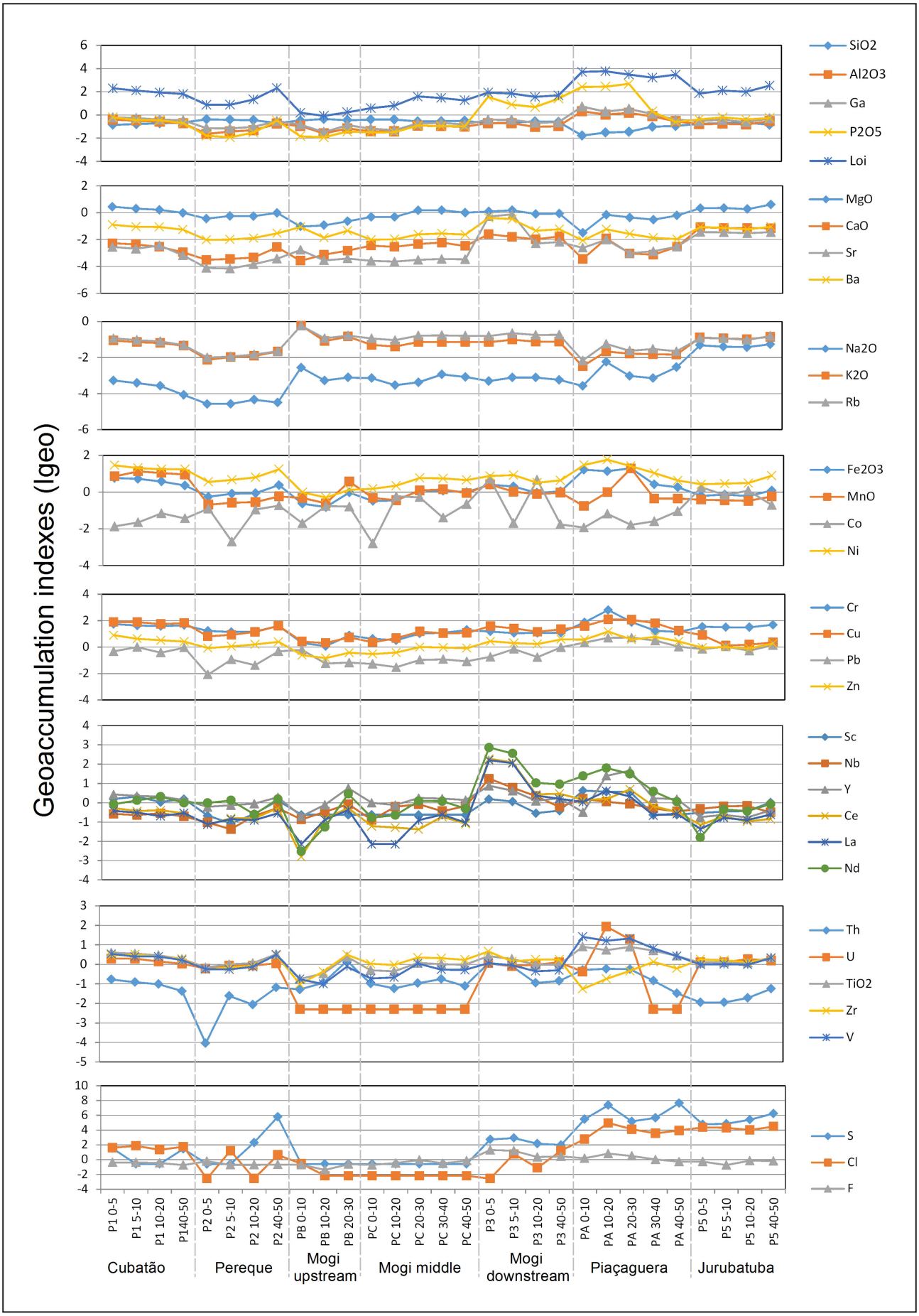

FIGURE 6. Geo-accumulation index of fluvial sediment cores of the upper estuarine system.

TABLE 4 - Classification of river sediment profiles from the upper Santos estuary by index of geoaccumulation (Igeo).

Igeo class	River Sediment Profile						
	Cubatão	**Pereque**	**Mogi upstream**	**Mogi middle**	**Mogi downstream**	**Piaçaguera**	**Jurubatuba**
1-unpolluted to moderately polluted: 0<Igeo<1	Fe,Mg,Mn,Nd,Sc	Cl,Cu,Fe,LOI,Nd,Ni	Cu,Cr,LOI,Mn,Nd,Ni	Cr,Cu,Fe,LOI,Mg,Mn	Ce,Cl,Co,F,Fe,La	Al,Ce,Ga,F,Fe,La	Co,Cu,Fe,Mg,Ni,Pb
	Ti,U,V,Y,Zn,Zr	Sc,Ti,U,V,Zn,Y,Zr	Th,Ti,Y,Zr	Nd,Ni,Ti,V,Y,Zr	Mg,Mn,Nb,Nd,Ni,P	Nb,Nd,Ni,P,Pb,Sc	Sc,Ti,U,V,Zn,Zr
					Sc,Th,Ti,U,V,Y,Zn,Zr	Y,Ti,V,Zn,Zr	
2-moderately polluted: 1<Igeo<2	Cl,Cr,Cu,LOI,Mn	Cl,Cr,Cu,LOI,Ni		Cr,Cu,LOI	Cl,Cr,Cu,F,LOI,Nb	Cr,Cu,Fe,Mn,Nd,Ni	LOI,Cr
	Ni,S				Nd,P,S	U,V,Y,Zn	
3-moderately to heavily polluted: 2<Igeo<3	LOI				Ce,La,Nd,S	Cl,Cr,Cu,P	LOI
4-heavily polluted: 3<Igeo<4		LOI,S				LOI,Cl	
5-heavily to extremely polluted: 4<Igeo<5						Cl	S,Cl
6-extremely polluted: Igeo>5		S				S	S

TABLE 5 - Association between paired samples, using one of Pearson's product moment correlation coefficient.

	Al	**Mn**	**Fe**	**LOI**	**Co**	**Cr**	**Cu**	**Ni**	**Pb**	**V**
Al										
Mn	0.54									
Fe	0.89	0.66								
LOI	0.85	0.22	0.80							
Co	-0.34	-0.34	-0.36	-0.20						
Cr	0.74	0.40	0.73	0.70	-0.21					
Cu	0.63	0.62	0.59	0.36	-0.47	0.55				
Ni	0.80	0.61	0.86	0.66	-0.39	0.84	0.73			
Pb	0.82	0.37	0.73	0.83	-0.28	0.67	0.40	0.61		
V	0.93	0.47	0.92	0.90	-0.31	0.78	0.51	0.83	0.80	
Zn	0.62	0.50	0.64	0.48	-0.40	0.64	0.86	0.76	0.54	0.55

represent the mineral predominance in the sediments, such as feldspars (sodic and potassic) and aluminum silicates, from the Ca-Mg minerals (amphiboles, carbonates, etc.).

The Mogi upstream and middle course rivers presented negative scores in the PC1, correlated to the Si, Mg and K elements (Fig. 9), in agreement with the field descriptions (Table 2) of the medium to coarse-grained sands with quartz, muscovite, feldspar, poorly selected and lytic fragments (Fig. 2A), and also the arkose/lithoarenite class of SandClass of the Herron classification (Fig. 3A). The Piaçaguera River sediments represent an independent group with strong positive scores in the PC1, principally related to P and LOI, in agreement to their field classification of the muddy swamp sediments, dark gray clay and high contents of organic matter, and classified in shale- Fe-shale in the SandClass of the Herron diagram (Fig. 3A), enriched in Al, Fe, Ti, P and LOI. The Jurubatuba River sediment samples represent a group enriched in Ca and Na, which are interpreted as a product of the tides at this point, related to mangrove deposits (Fig. 2C). These sediments had the highest contents of Ca, Na, S and Cl (Table 3).

The PC1 for the trace elements explain 43.2% of the total variance and have positive loading (>0.5) on La, Ce, Sr, Nb, Nd and F. This PC is the most important component which explained the anthropogenic source. These elements are enriched in phosphogypsum waste samples (Table 3). The other industries (fossil fuels, metallurgical, chemical, etc.), and also urban/domestic pollutes in the watershed area can contribute to Ni, Cr, Cu, V, Zn and Pb pollutants, which were grouped with negative loading in the PC1 (Fig. 9).

The Mogi downstream sediments represent an independent group with strong positive scores in the PC1 related to enrichment in the La, Ce, Sr, Nb, Nd and F elements. This suggests that these elements are mainly of anthropogenic origin (phosphogypsum waste) in the Mogi downstream river.

4.2. Anthropogenic sources

Soil quality criteria and guiding values in Brazil do not address fluvial sediments. The National Environment Council contains a resolution for assessment of the material to be dredged in Brazilian jurisdictional waters. However, it only addresses 8 metals (As, Cd, Pb, Cu, Cr, Hg, Ni and Zn), but elements associated with other polluting sources, such as phosphogypsum waste, are not considered (e.g. Ce, La, Nd and F). In addition, aqua regia digestion methods are used to leach metals that are adsorbed into minerals, with a focus on biotoxicity. This work used the total extraction method; thus, it cannot be appropriately compared with the Brazilian guiding values.

Furthermore, the definitions and use of the term "background" in exploration and environmental geochemistry is fraught with problems. The background may change from area to area within a region and between regions. Therefore, it is important to recognize that background depends on location and scale, and such values are a range, not a single value. Geochemical mapping on many different scales will be necessary to determine site-specific backgrounds and to provide full insights into the processes that cause deviations from the background (Reimann and Garret 2005).

Thus, for characterization of contaminated sediments, a sampling of sediments, soils and rocks on a hydrographic basin scale is recommended, with a set of samples that provides a multivariate statistical analysis of the data. In this sense, the results allow some considerations in relation to the groups of chemical elements and their probable mineral or anthropic sources.

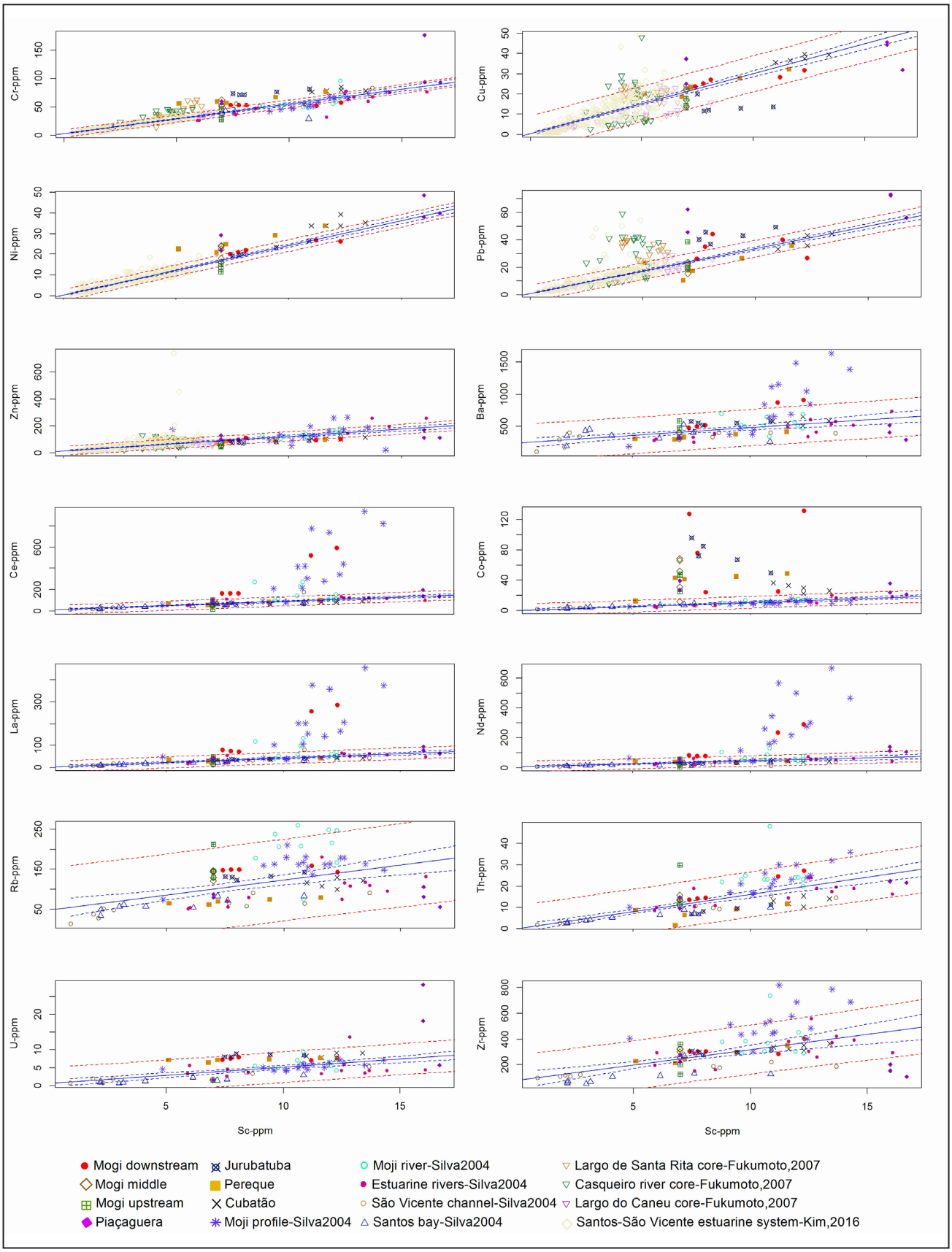

FIGURE 7. Scatterplot showing the relationship between selected elements and the Sc grain-proxy element.

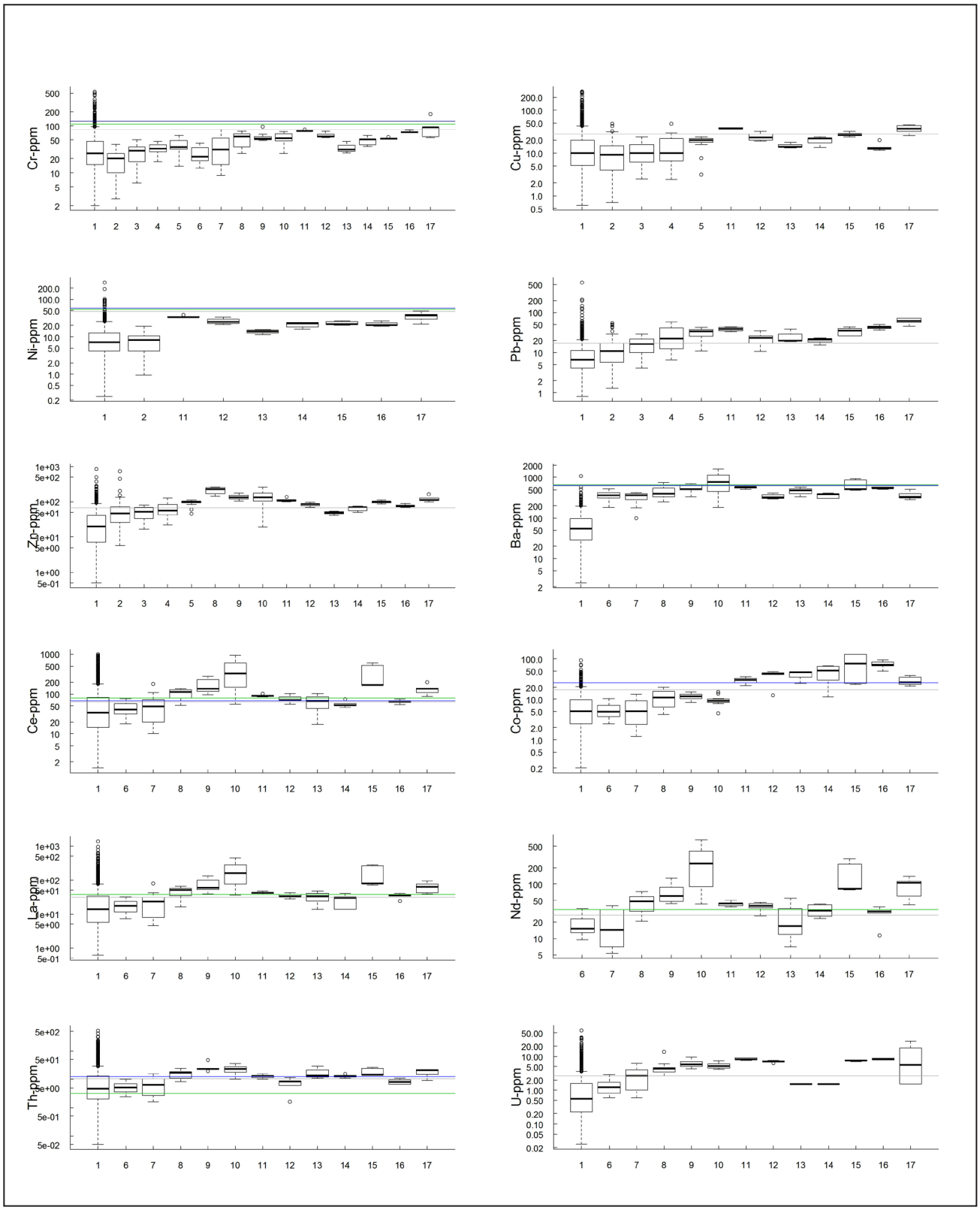

FIGURE 8. Boxplots of selected elements in sediments of the: 1: stream sediment geochemistry data on a low-density sampling scale in the State of São Paulo (Mapa 2015); 2: Santos-São Vicente estuary (Kim 2016); 3: Largo do Caneu sediment core, 4: Casqueiro sediment core, and 5: Largo de Santa Rita sediment-core, in the Santos estuary (Fukumoto 2007); 6: Santos Bay, 7: São Vicente channel, 8: Estuarine rivers, 9: Mogi river and 10: sediment core in the Mogi river (Silva 2004); 11: Cubatão, 12: Pereque, 13: Mogi upstream, 14: Mogi middle, 15: Mogi downstream, 16: Jurubatuba and 17: Piaçaguera rivers (this study). Blue line: NASC; Gray line: UCC; Green line: PASS.

TABLE 6 - Principal component analysis of the selected elements in the fluvial sediment samples along the upper portion of the Santos-São Vicente estuarine system (n=30).

PCA	PC-1	PC-2	PC-3	PC-4	PC-5	PC-6	PC-7	PC-8	PC-9	PC-10	KMO
Major elements											
Eigenvalue	5.2	2.8	1.0	0.8	0.5	0.2	0.1	0.1	0.0	0.0	
Contribution	48.8	26.6	9.0	7.9	4.2	1.7	0.8	0.6	0.2	0.2	
Si	-0.60	-0.65	0.13	0.18	0.33	0.08	0.12	0.00	0.05	-0.03	0.62
Al	0.82	-0.12	0.47	0.09	-0.09	0.13	-0.12	0.04	-0.01	-0.07	0.69
Mn	0.00	-0.75	-0.13	-0.50	-0.35	-0.08	0.05	0.05	0.02	-0.02	0.65
Mg	-0.70	-0.36	-0.43	0.32	-0.19	0.14	-0.04	-0.05	-0.07	-0.01	0.26
Ca	-0.77	0.47	-0.31	0.11	0.03	-0.12	-0.15	0.05	0.07	-0.03	0.28
Na	-0.55	0.60	0.47	0.11	-0.22	-0.15	0.07	-0.09	-0.02	-0.01	0.70
K	-0.81	-0.34	0.37	-0.19	0.06	0.07	-0.11	0.05	-0.02	0.08	0.73
Ti	0.62	-0.60	0.01	0.35	0.11	-0.28	-0.02	0.06	-0.05	0.01	0.72
P	0.63	0.53	-0.22	-0.40	0.28	0.02	0.01	-0.01	-0.05	-0.01	0.51
Fe	0.84	-0.47	-0.08	0.02	0.01	-0.01	-0.08	-0.17	0.05	0.03	0.61
LOI	0.80	0.37	-0.11	0.32	-0.19	0.12	0.08	0.08	0.04	0.05	0.63
Minor elements											
Eigenvalue	5.9	3.2	1.7	0.9	0.8	0.7	0.4	0.3	0.2	0.2	
Contribution	40.7	21.8	11.6	6.5	5.8	4.5	3.1	2.0	1.2	1.1	
Ba	-0.04	-0.73	0.12	-0.53	0.25	0.16	-0.12	0.15	0.02	-0.08	0.76
Ce	0.71	0.56	-0.11	-0.16	-0.11	0.01	0.12	0.03	0.04	0.24	0.79
Co	0.20	-0.70	0.42	0.16	-0.39	0.13	0.09	-0.23	-0.03	-0.04	0.49
Cr	-0.84	-0.13	-0.12	0.16	-0.15	0.20	-0.31	-0.02	-0.07	0.07	0.62
Cu	-0.69	0.42	0.29	-0.18	0.14	0.03	0.36	0.03	-0.18	0.00	0.78
F	0.43	-0.03	0.17	0.54	0.66	0.13	-0.02	-0.04	-0.07	0.01	0.85
La	0.75	0.48	-0.21	-0.18	-0.08	0.08	0.00	-0.03	-0.17	-0.17	0.86
Nb	0.51	-0.48	0.48	0.20	-0.09	-0.30	0.14	0.26	0.07	0.00	0.84
Nd	0.49	0.78	-0.05	0.16	-0.05	0.05	-0.14	0.08	0.17	-0.14	0.80
Ni	-0.91	0.14	0.06	0.02	-0.01	0.17	-0.01	0.25	0.02	-0.03	0.71
Pb	-0.55	-0.24	-0.56	-0.02	0.17	-0.46	0.10	-0.13	0.06	-0.10	0.73
Sr	0.52	-0.57	-0.55	-0.09	0.13	0.04	-0.02	0.04	-0.02	0.14	0.70
V	-0.83	0.13	-0.17	0.26	-0.17	-0.23	-0.07	0.12	-0.11	0.03	0.71
Y	-0.28	0.39	0.65	-0.29	0.19	-0.29	-0.28	-0.15	0.02	0.07	0.68
Zn	-0.86	0.10	-0.05	0.01	0.10	0.26	0.22	-0.12	0.22	0.02	0.86

The techniques of: (i) data normalized with the upper continental crust (UCC); (ii) index of geoaccumulation (Igeo) with background of the mean regional rocks; (iii) prediction and confidence intervals from robust regression analysis (RA), together with compiled regional geochemical data; (iv) principal component analysis and (v) metal/aluminum ratios relationships, were useful for understanding the geochemical data on a watershed scale. The UCC-normalized and Igeo values indicated that elements are enriched in relation to a continental reference value and a regional geological substrate, respectively. It demonstrated that Co and Pb can be of natural origin, with naturally enriched rock (Fig. 6). The use of robust linear regression to eliminate the grain size effect, from a larger number of samples compiled on a local to a regional scale, showed occasional lead anomalies in the Jurubatuba, Mogi dowstream and Piaçaguera rivers (Fig. 7). This reinforces the importance of low-density geochemical surveys throughout the national territory as a support for the definition of baseline values.

The PCA scores exhibit strong spatial association with known locations of industrial waste and potential polluting industries. PC1 loading separated heavy metals (Cr, Cu, Ni, Pb, V and Zn) from the elements that are probably associated with the phosphogypsum waste (Ce, La, Sr, Nd, Nb and F). The PC scores, UCC-normalized data and Igeo values in the Mogi downstream River showed anomalous results for the Ce, La, Sr, Nd, Nb and F, which are likely to have an anthropogenic source. The plots of PC1 and PC2 (loading and scores) grouped Cu, Ni, V and Zn related to the Cubatão, Pereque and Piaçaguera rivers. Industrial waste deposits and contaminated soil were mapped in this region (CETESB 2001), and so was the presence of chemical industries and oil refineries (Fig. 1); however, it was not possible to characterize a single source of this anomalous results.

The metal/aluminum ratios minimize the sediment grain-size effect and have been proposed as potential discriminant proxies for sediment sources (Grant and Middleton 1998; Jung et al. 2016). The ratios of the sediment cores are compared to

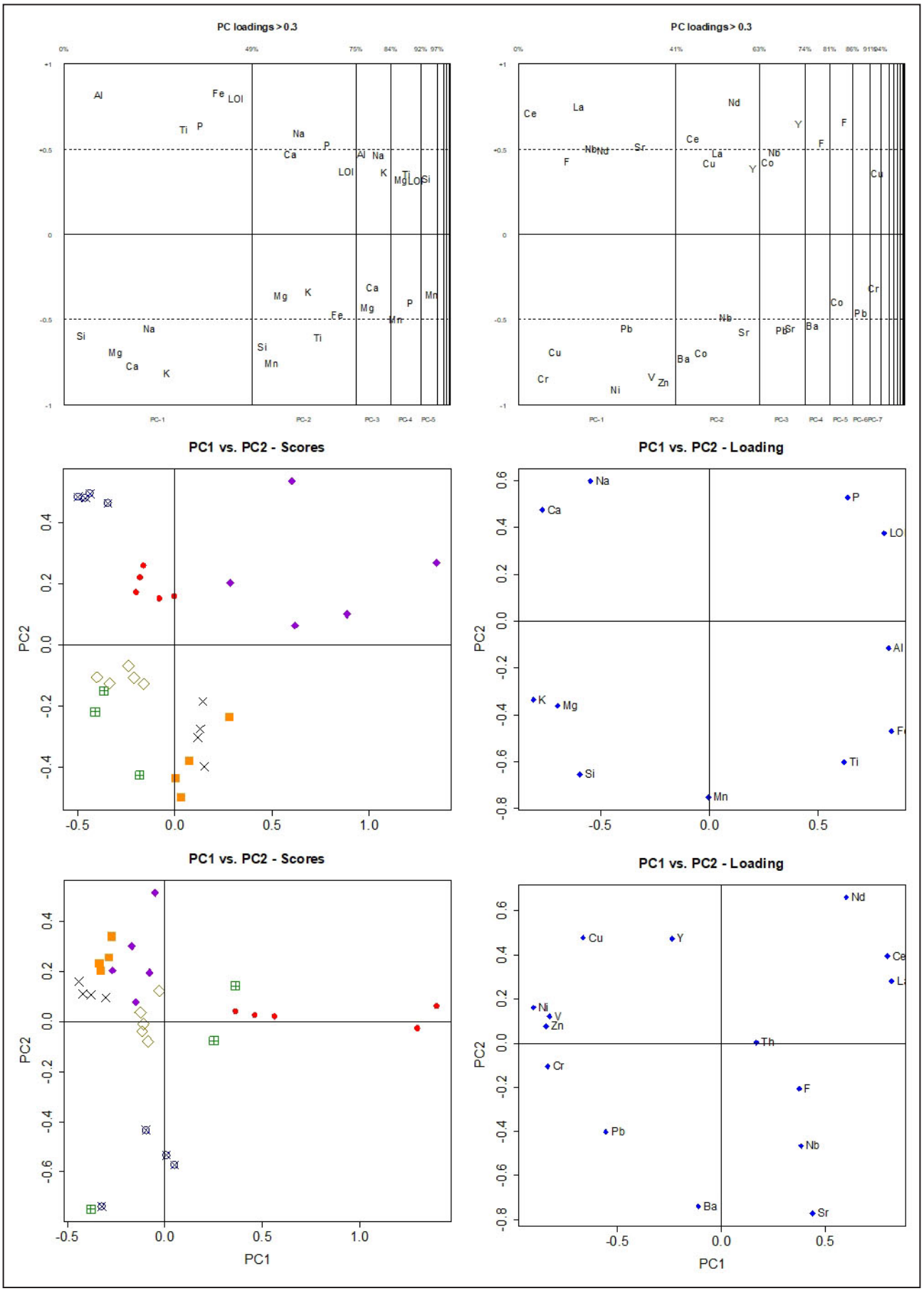

FIGURE 9. PCA loading and scores plots obtained for the data set

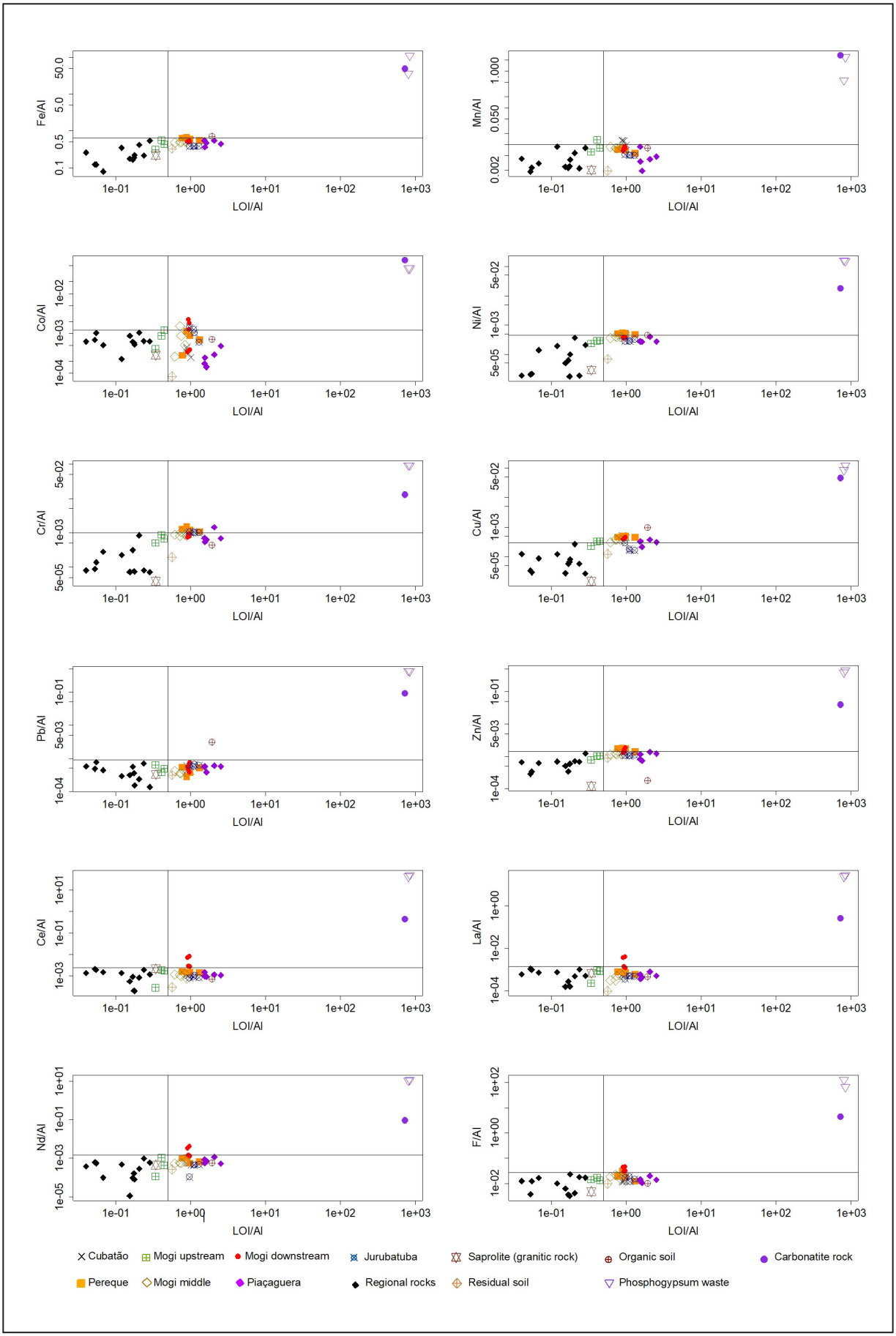

FIGURE 10. Metal/aluminum versus LOI/Al ratios of sedimentary cores compared to phosphogyspum waste, soils and regional rocks.

the phosphogypsum waste, soils and regional rocks as “end members” to be distinguished from anthropogenic sources (Fig. 10). The LOI/Al ratio was chosen because of its potential to distinguish more clayey sediments with higher concentrations of organic matter. The results showed higher metal/aluminum ratios of the phosphogypsum waste and carbonatite rock. The vertical and horizontal lines delimit the field of regional rocks, saprolite rock, residual soil and Mogi upstream sediments (Fig. 10). We interpret that the horizontal line represents the maximum metal/aluminum ratio for the geogenic sources (regional rocks and residual soil). Values above this threshold are characterized as enriched and probably have an anthropogenic source (Fig. 10). The sediments of the Piaçaguera River showed high levels of heavy metals (Cr, Cu, Ni, Pb and Zn), classified as moderately to heavily polluted according to the IGeo values (Table 6). However, metal/aluminum ratios showed only anomalous values for Cr and Cu.

5. Conclusion

Major and trace element geochemistry of the upper estuarine sediments of the Santos estuary and its possible source materials (soils and rocks) demonstrated that the phosphogypsum waste deposited on the banks of the hydrographic basin of the Mogi and Piaçaguera rivers affected the chemical conditions of these rivers. The concentrations of P, S, F, Nd, Ce, La, Nb, Th and Y in the Mogi downstream river sediments can be directly related to sources of phosphogypsum waste pollution.

The statistical techniques proposed in this study are complementary. The Igeo indices showed elements of probable anthropogenic origin, when compared to lithology on a local scale. UCC-normalized data indicate enrichment compared to references on a continental scale. The Robust Linear Regression method showed which elements are enriched, when compared to a larger number of samples on a regional scale. The geochemical assessment on a local, regional and continental scale has reinforced the importance of geochemical surveys throughout the Brazilian territory, as a geochemical reference database. The APC analysis showed the main groups of interrelated chemical elements (factor loading) and the sample scores on these factors (factor scores), which allows the assessment of the samples and chemical elements related to an anthropic origin. Finally, Metal/Al ratios eliminated the sediment texture effects and suggest the presence of end-members of anthropogenic and geogenic sources, which complement the analysis of provenance of the anthropogenic contaminants.

The Chemical Index of Alteration (CIA) and A-CN-K ternary diagram indicated that the upper estuarine sediments display a wide range of weathering effects, from unweathered upper crust derived of Proterozoic gneiss and granitic rocks to intensely weathered site in swamp deposits of the Piaçaguera River. Among the major elements, the APC analysis showed a spatial association with types of weathering and sedimentary deposits. The projection of components 1 and 2 (factor loading and factor scores) allowed a separation of the main rock-forming elements (Si, Mg and K) from the mobile elements (Ca, Na and P) and from the immobile elements (Al, Fe, Ti). For example, the sediments of the Mogi upstream river are classified as arkose/litharenite, enriched in Si, Mg and K (immature sediments), while swamp deposits of the Piaçaguera river are classified into shale/Fe-shale, enriched with organic matter, P, Al, Fe and lower Si contents. The higher CIA values and the A-CN-K diagram for the Piaçaguera sediments indicated intense weathering, which may suggest the important role of the tides in modifying the present minerals, or even represent Holocene intertidal beach sediments from the marine regression process.

Acknowledgments

We would like to thank the anonymous reviewers for helping us to improve this manuscript. We are thankful to Felipe Costa’s review of the previous version of the manuscript.

6. References

Abbas M., Bruns R., Scarminio I., Ferreira J. 1993. A Multivariate Statistical Analysis of the Compositions of Rainwater near Cubatão, SP, Brazil. Environmental Pollution, 79, 225-233. https://doi.org/10.1016/0269-7491(93)90094-5

Aitchison J. 1986. The statistical analysis of compositional data. London, UK: Chapman & Hall, Ltd. https://doi.org/10.1002/bimj.4710300705

Alves A., Janasi V., Campos Neto M., Heaman L., Simonetti A. 2013. U–Pb geochronology of the granite magmatism in the Embu Terrane: Implications for the evolution of the Central Ribeira Belt, SE Brazil. Precambrian Research, 230, 1-12. https://doi.org/10.1016/j.precamres.2013.01.018

Bauer A., Velde B.D. 2014. Geochemistry at the earth’s surface - movement of chemical elements. New York: Springer-Verlag Berlin Heidelberg. 315 p. DOI: 10.1007/978-3-642-31359-2

Bontempi E. 2020. First data analysis about possible COVID-19 virus airborne diffusion due to air particulate matter (PM): the case of Lombardy (Italy). Environment Research, 186, 109639. https://doi.org/10.1016/j.envres.2020.109639

Borges R.M.M. 2003. Caracterização do fosfogesso dos depósitos do pólo industrial de Cubatão e investigação confirmatória da contaminação das águas subterrâneas. MSc Dissertation, Escola Politecnica, Universidade de São Paulo, São Paulo. https://repositorio.usp.br/item/001344181

Borrego E., Mas J., Martín J., Bolívar J., Vaca F., Aguado J. 2007. Radioactivity levels in aerosol particles surrounding a large TENORM waste repository after application of preliminary restoration work. Science of the Total Environment, 377, 27-35. https://doi.org/10.1016/j.scitotenv.2007.01.098

Bourg A. 1988. Metals in aquatic and terrestrial systems: sorption, speciation, and mobilization. In: Salomons W., Förstner U. (eds.). Chemistry and biology of solid waste. Berlin Heidelberg: Springer-Verlag. p. 3-32. https://link.springer.com/book/10.1007/978-3-642-72924-9

Calado B.O. 2008. Geoquímica elemental e isotópica Sr e Nd como traçadores de poluentes Antrópicos, Caso de Estudo: Fosfogesso de Cubatão. MSc Dissertation, Instituto de Geociências, Universidade de São Paulo, São Paulo. 114p. DOI: 10.11606/D.44.2008.tde-19082008-082411

CETESB. 1985. Qualidade do ar na região metropolitana de São Paulo e em Cubatão. https://cetesb.sp.gov.br/qualidade-ar/wp-content/uploads/sites/28/2013/12/1985.pdf

CETESB. 2001. Sistema estuarino de Santos e São Vicente . Technical Report. São Paulo: CETESB. DOI: 10.13140/RG.2.1.3288.9764

CETESB. 2018. Fluoreto atmosférico na região de Cubatão: biomonitoramento da vegetação e taxas atmosféricas 2016. Série Relatórios. São Paulo: CETESB. Available online at: http://cetesb.sp.gov.br/ar/publicacoes-relatorios/ (accessed on 13 June 2020).

Chieregati L., Silva A., Ostafiuc G., Filho J., Alegri V., Silva V. 1991. Projeto integração geológica da Região Metropolitana de São Paulo. Relatório de Integração Geológica: relatório final. São Paulo: CPRM. 2v. http://rigeo.cprm.gov.br/jspui/handle/doc/8761

Fávaro D.I.T. 2005. Distribution of U and Th decay series and rare earth elements in sediments of Santos Basin: Correlation with industrial activities. Journal of Radioanalytical and Nuclear Chemistry, 264, 449-455. https://doi.org/10.1007/s10967-005-0736-3

Förstner U., Ahlf W., Calmano W., Kersten M. 1990. Sediment Criteria Development. In: Heling D., Rothe P., Förstner U., Stoffers P. (eds.). Sediments and Environmental Geochemistry. Springer, Berlin, Heidelberg. p. 311-338. https://doi.org/10.1007/978-3-642-75097-7_18

Fukumoto M.M. 2007. Determinação da história deposicional recente do Alto Estuário Santista, com base nos teores de metais e na suscetibilidade magnética dos sedimentos. PHD Thesis, Instituto Oceanográfico, Universidade de São Paulo. DOI: 10.11606/T.21.2007.tde-06112007-110644

Furlan C.M. 1998. Efeitos da poluição aérea de Cubatão sobre o conteúdo de nitrogênio, fibras, ligninas e substâncias fenólicas foliares e atividade herbivórica em Tibouchina pulchra Cogn.. MSc Dissertation. Instituto de Biociências, Universidade de São Paulo, São Paulo. DOI: 10.11606/D.41.1998.tde-27042005-112012

Gao X., Li P. 2012. Concentration and fractionation of trace metals in surface sediments of intertidal Bohay Bay, China. Marine Pollution Bulletin, 64, 1529-1536. https://doi.org/10.1016/j.marpolbul.2012.04.026

Garzanti E., Andó S., France-Lanord C., Censi P., Vignola P., Galy V., Lupker M. 2011. Mineralogical and chemical variability of fluvial sediments 2. Suspended-load silt (Ganga–Brahmaputra, Bangladesh). Earth and Planetary Science Letters, 302, 107-120. https://doi.org/10.1016/j.epsl.2010.11.043

Grant A., Middleton R. 1998. Contaminants in sediments: using grain-size normalization. Estuaries, 21, 197-203. https://doi.org/10.2307/1352468

Guo Y., Yang S., Su N., Li C., Yin P., Wanf Z. 2018. Revisiting the effects of hydrodynamic sorting and sedimentary recycling on chemical weathering indices. Geochimica et Cosmochimica Acta, 227, 48-63. https://doi.org/10.1016/j.gca.2018.02.015

Gutberlet J. 1997. Cubatão: desenvolvimento, exclusão social e degradação ambiental. São Paulo: EDUSP. ISBN 9788531403552.

Hasui Y., Dantas A., Carneiro C., Bistrichi C. 1981. O embasamento Pré-Cambriano e Eopaleozóico em São Paulo. In: Almeida F.F.M., Hasuy Y., Ponçano W.L. et al. Mapa Geológico do Estado de São Paulo: IPT. Escala 1:500.000. p. 12-45.

Heilbron M., Valeriano C., Tassinari C., Almeida J., Tupinambá M., Siga Jr. O., Trouw R. 2008. Correlation of Neoproterozoic terranes between the Ribeira Belt, SE Brazil and its African counterpart: comparative tectonic evolution and open questions. In: Pankhurst R., Trouw R., Brito Neves B., De Wit M. West Gondwana: Pre-Cenozoic correlations across the South Atlantic Region. Geological Society, London, Special Publications, 294, 211-237. http://dx.doi.org/10.1144/SP294.12

Herron M. 1988. Geochemical classification of Terrigenous Sands and Shales from Core or Log Data. Journal of Sedimentary Petrology, 58, 820-829. http://dx.doi.org/10.1306/212F8E77-2B24-11D7-8648000102C1865D

IPEN. 1986. Caracterização química das águas da chuva de Cubatão. Projeto n. INPE-3965-RPE/515. Instituto de Pesquisas Espaciais.

Jacomino V., Oliveira K., Taddei M., Siqueira M., Carneiro E., Nascimento M., Mello J. 2009. Radionuclies and Heavy Metal Contents in Phosphogypsum Samples in Comparison to Cerrado Soils . Revista Brasileira de Ciência do Solo, 33, 1481-1488. https://doi.org/10.1590/S0100-06832009000500038

Jenne E.A. 1968. Controls on Mn, Fe, Co, Ni, Cu and Zn concentrations in soils and water: the significant role of hydrous Mn and Fe oxides. In: Gould, R.F. (ed.). Trace Inorganics in Water. American Chemical Society. v. 73, p. 337-387. DOI: 10.1021/ba-1968-0073.ch021

Jolliffe I.T. 2002. Principal component analysis. Springer-Verlag New York. 518p. DOI: 10.1007/b98835

Jung H., Lim D., Jeong D., Xu Z., Li T. 2016. Discrimination of sediment provenance in the Yellow Sea: Secondary grain-size effect and REE proxy. Journal of Asian Earth Sciences, 123. p. 78-84. http://dx.doi.org/10.1016/j.jseaes.2016.03.020

Kaiser H.F. 1974. An index of factor simplicity. Psychometrika, 39, 1, p. 31-36. Available on line at: https://link.springer.com/article/10.1007/BF02291575 (accessed on 7 January 2020)

Kim B. 2016. Índices de qualidade ambiental para avaliação de metais e semimetais em sedimentos do complexo estuarino de Santos e São Vicente SP, Brasil. MSc Dissertation. Instituto Oceanográfico, Universidade de São Paulo, São Paulo. DOI: 10.11606/D.21.2017.tde-06072017-154448

Kim B., Angeli J., Ferreira P., Mahiques M., Figueira R. 2018 . Critical evaluation of different methods to calculate the Geoaccumulation Index for environmental studies: A new approach for Baixada Santista – Southeastern Brazil. Marine Pollution Bulletin, 127, 548–552. https://doi.org/10.1016/j.marpolbul.2017.12.049

Kim B., Angeli J., Ferreira P., Sartoretto J., Miyoshi C., Mahiques M., Figueira R. 2017. Use of a chemometric tool to establish the regional background and assess trace metal enrichment at Baixada Santista e southeastern Brazil. Chemosphere, 166, 372-379. https://doi.org/10.1016/j.chemosphere.2016.09.132

Klumpp A., Domingos M., Klumpp G. 1996. Assessment of the vegetation risk by fluoride emissions from fertiliser industries at Cubatão, Brazil. The Science of the Total Environment, 192, 219-228. https://doi.org/10.1016/S0048-9697(96)05298-9

Lü H., Huang Y., Huang X., Cai Q. 2019. The state of particulate matter contamination, particulate matter–bound heavy metals, and persistent organic pollutants POPs in megacities, China. Current Opinion in Environmental Science & Health, 8, 15-22. https://doi.org/10.1016/j.coesh.2019.01.001

Luoma S.N. 1990. Process affecting metal concentrations in estuarine and coastal marine sediments. In: Furness R.W., Rainbow P.S. (eds.) Heavy Metals in the Marine Environment. Taylor & Francis Group. p. 51-62.

Manceau A., Lanson M., Geoffroy N. 2007. Natural speciation of Ni, Zn, Ba and As in ferroman- ganese coatings on quartz using X-ray fluorescence, adsorption and diffraction. Geochimica et Cosmochimica Acta, 71, 95-128. https://doi.org/10.1016/j.gca.2006.08.036

Mapa F. 2015. Geoquímica multielement ar d e sedimentos de corrente no estado de São Paulo: abordagem através da análise estatística multivariada. MSc Dissertation. Instituto de Geociências, Universidade de São Paulo, São Paulo. DOI: 10.11606/D.44.2016.tde-17062016-144236

Maronna R.A., Martin R.D., Yohai V.J., Salibián-Barrera M. 2019. Robust Statistics: Theory and Methods (with R). John Wiley & Sons Ltd. 430p.

McLennan S., Hemming S., McDaniel D., Hanson G. 1993. Geochemical approaches to sedimentation, provenance and tectonics. In: Johnsson M., Basu A. Processes controlling the composition of clastic sediments. Colorado: Geological Society of America Special Paper, 284. p. 21-40. http://dx.doi.org/10.1130/SPE284-p21

Means J., Crerar D., Duguid J. 1978. Migration of Radioactive Wastes: Radionuclide Mobilization by Complexing Agents. Science, 200, 1477-1481. DOI: 10.1126/science.200.4349.1477

Meira V., Garcia-Casco A., Juliani C., Schorscher J. 2019. Late Tonian within-plate mafic magmatism and Ediacaran partial melting and magmatism in the Costeiro Domain, Central Ribeira Belt, Brazil. Precambrian Research, 334, 1-22. https://doi.org/10.1016/j.precamres.2019.105440

Modak D., Singh, K. Chandra H., Ray P. 1992. Mobile and bound forms of trace metals in sediments of the lower Ganges. Water Research, 26, 1541-1548. https://doi.org/10.1016/0043-1354(92)90075-F

Müller G. 1969. Index of geoaccumulation in sediments of the Rhine River. GeoJournal, 2, 108-118.

Nesbitt H., Young G. 1982. Early proterozoic climates and plate motions inferred from major element chemistry of lutites. Nature, 299, 715-717. https://doi.org/10.1038/299715a0

Nichols G. 2009. Sedimentology and Stratigraphy. Garsington Road, Oxford, UK: A John Wiley & Sons, Ltd., Publication. Available on line at: https://raregeologybooks.files.wordpress.com/2014/09/sedimentology-and-stratigraphy-by-gary-nichols.pdf (accessed on 7 January 2020)

Ogundele L., Owoade O., Hopke P., Olise F. 2017. Heavy metals in industrially emitted particulate matter in Ile-Ife, Nigeria. Environmental Research, 156, 320-325. https://doi.org/10.1016/j.envres.2017.03.051

Okbah M., Nasr S., Soliman N., A.M. 2014. Distribution and Contamination Status of Trace Metals in the Mediterranean Coastal. Sediments, Egypt, Soil and Sediment Contamination: An International Journal, 23, 6, 656-376. https://doi.org/10.1080/15320383.2014.851644

Oliveira S., Silva P., Mazzilli B., Favaro D., Saueia C. 2007. Rare earth elements as tracers of sediment contamination by phosphogypsum in the Santos estuary, southern Brazil. Applied Geochemistry, 22, 837-850. https://doi.org/10.1016/j.apgeochem.2006.12.017

Pang H., Pan B., Garzanti E., Gao H., Zhao X., Chen D. 2018. Mineralogy and geochemistry of modern Yellow River sediments: Implications for weathering and provenance. Chemical Geology, 488, 76-86. http://dx.doi.org/10.1016/j.chemgeo.2018.04.010

Papaslioti E., Pérez-López R., Parviainen A., Phan V., Marchesi C., Fernandez-Martinez A., Charlet L. 2020. Effects of redox oscillations on the phosphogypsum waste in an estuarine salt-marsh system. Chemosphere, 242. https://doi.org/10.1016/j.chemosphere.2019.125174

Pires F. 2012. "Vale da morte" foi o símbolo de Cubatão. Valor Econômico. Available on line at: https://valor.globo.com/brasil/noticia/2012/03/15/

vale-da-morte-foi-o-simbolo-de-cubatao.ghtml (accessed on10 February 2020)

Reimann C., Garrett R. 2005. Geochemical background - concept and reality. Science of the Total Environment, 350, 12-27. https://doi.org/10.1016/j.scitotenv.2005.01.047

Rizzio E., Bergamaschi L., Valcuvia M., Profumo A., Gallorini M. 2001. Trace elements determination in lichens and in the airborne particulate matter for the evaluation of the atmospheric pollution in a region of northern Italy. Environment International, 26, 543-549. DOI: 10.1016/s0160-4120(01)00037-x

Rodrigues Filho S., Maddock J. 1997 . Mercury pollution in two gold mining areas of the Brazilian Amazon. Journal of Geochemical Exploration, 58, 231-240. https://doi.org/10.1016/S0375-6742(97)00006-X

Rousseeuw P.J., Leroy A.M. 1987. Robust regression and outlier detection. United States of America: John Wiley & Sons, Inc. DOI:10.1002/0471725382

Roy P., Caballero M., Lozano R., Smykatz-Kloss W. 2008. Geochemistry of late quaternary sediments from Tecocomulco lake, central Mexico: Implication to chemical weathering and provenance. Geochemistry, 68, 383-393. https://doi.org/10.1016/j.chemer.2008.04.001

Santos A., Mazzilli B., Favaro D. 2002. Characterization of stockpiled phosphogypsum waste in Santos basin, Brazil. Radioprotection, 37, 1307-1315. https://doi.org/10.1051/radiopro/2002165

Schropp S., Lewis W. H., Ryan J., Calder F., Burney L. 1990. Interpretation of Metal Concentrations in Estuarine Sediments of Florida Using Aluminum as a Reference Element. Estuaries, 13, 227-235. https://doi.org/10.2307/1351913

Silva A., Filho C., Chiodi D., Filho W. 1977. Projeto Santos-Iguape. Geologia: relatório fina. São Paulo: CPRM. http://rigeo.cprm.gov.br/jspui/handle/doc/9506

Silva P. 2004. Caracterizacao quimica e radiologica dos sedimentos do estuario de Santos, São Vicente e Baia de Santos. PhD Thesis. Instituto de Pesquisas Energéticas e Nucleares - Ipen. São Paulo, SP. http://repositorio.ipen.br:8080/xmlui/handle/123456789/11215

Spektor D.M., Hofmeister V.A., Artaxo P., Brague J.A.P., Echelar F., Nogueira D.P., Hayes C., Thurston G.D., Lippmann M., 1991. Effects of Heavy Industrial Pollution on Respiratory Function in the Children of Cubatao, Brazil: a preliminary report. Environmental Health Perspectives, 94, 51-54. https://doi.org/10.1289/ehp.94-1567962

Suguio K., Martin L., Fairchild T. 1978. Quaternary Marine Formations of the State of São Paulo and Southern Rio de Janeiro. In: International Symposium on Coastal Evolution in the Quaternary. São Paulo - Brasil: Instituto de Geociências – USP. Available on line at: https://core.ac.uk/download/pdf/39879155.pdf (accessed on14 March 2020)

Tagawa P., Moruzzi D., Cury J. 2009. Fluoride concentration in the adjacent vegetation next to fertilizer industries of Cubatão, São Paulo, Brazil. Ciência & Saúde Coletiva, 14, 2205-2208. https://doi.org/10.1590/S1413-81232009000600028

Taylor S., McLennan S. 1985. The Continental Crust: Its Composition and Evolution. Oxford: Blackwell.

Torres-Sánchez R., Sánchez-Rodas D., Campa A., Rosa J. 2020. Hydrogen fluoride concentrations in ambient air of an urban area based on the emissions of a major phosphogypsum deposit SW, Europe. Science of The Total Environment, 714. https://doi.org/10.1016/j.scitotenv.2020.136891

Varol M. 2011. Assessment of heavy metal contamination in sediments of the Tigris River Turkey using pollution indices and multivariate statistical techniques. Journal of Hazardous Materials, 195, 355-364. https://doi.org/10.1016/j.jhazmat.2011.08.051

Vásconez-Maza M., Martíne-Segura M., Bueso M., Faz A., García-Nieto C., Gabarrón M., Acosta J. 2019. Predicting spatial distribution of heavy metals in an abandoned phosphogypsum pond combining geochemistry, electrical resistivity tomography and statistical methods. Journal of Hazardous Materials, 374, 392-400. https://doi.org/10.1016/j.jhazmat.2019.04.045

Vieira-Filho M. L. 2015. Influence of local sources and topography on air quality and rainwater composition in Cubatão and São Paulo, Brazil. Atmospheric Environment, 101, 200-208. https://doi.org/10.1016/j.atmosenv.2014.11.025

Wedepohl K. 1995. The composition of the continental crust. Geochimica et Cosmochimica Acta, 59, 1217-1232. https://doi.org/10.1016/0016-7037(95)00038-2

Wei Z, Wang D., Zhou H., Qi Z. 2011. Assessment of soil heavy metal pollution with principal component analysis and geoaccumulation index. Procedia Environmental Sciences, 10, Part c, 1946-1952. https://doi.org/10.1016/j.proenv.2011.09.305

Yohai V.J. 1987. High breakdown-point and high efficiency estimates for regression. The Annals of Statistics, 15, 642-65. https://www.jstor.org/stable/2241331

Yohai V.J., Stahel W.A., Zamar R. 1991. A procedure for robust estimation and inference in linear regression. In: Stahel, Weisberg (eds.). Directions in Robust Statistics and Diagnostics, Part II, New York, Springer, p. 365-374. https://doi.org/10.1007/978-1-4612-4444-8_20

Zhang P., Zhou X. 2020. Health and economic impacts of particulate matter pollution on hospital admissions for mental disorders in Chengdu, Southwestern China. Science oh the Total Environment, 733, 139114. https://doi.org/10.1016/j.scitotenv.2020.139114